

Nested Vehicle Routing Problem: Optimizing Drone-Truck Surveillance Operations

Fanruiqi Zeng^{*,1}, Zaiwei Chen¹, John-Paul Clarke² and David Goldsman³

ARTICLE INFO

Keywords:

aerial surveillance
cooperative vehicle routing
mixed integer programming
persistent operation
unmanned aerial vehicle

ABSTRACT

Unmanned aerial vehicles or drones are becoming increasingly popular due to their low cost and high mobility. In this paper we address the routing and coordination of a drone-truck pairing where the drone travels to multiple locations to perform specified observation tasks and rendezvous periodically with the truck to swap its batteries. We refer to this as the Nested-Vehicle Routing Problem (Nested-VRP) and develop a Mixed Integer Programming (MIP) formulation with critical operational constraints, including drone battery capacity and synchronization of both vehicles during scheduled rendezvous. Given the NP-hard nature of the Nested-VRP, we propose an efficient neighborhood search (NS) heuristic where we generate and improve on a good initial solution (i.e., where the optimality gap is on average less than 6% in large instances) by iteratively solving the Nested-VRP on a local scale. We provide comparisons of both the MIP and NS heuristic methods with a relaxation lower bound in the cases of small and large problem sizes, and present the results of a computational study to show the effectiveness of the MIP model and the efficiency of the NS heuristic, including for a real-life instance with 631 locations. We envision that this framework will facilitate the planning and operations of combined drone-truck missions.

1. Introduction

Unmanned aerial vehicles, commonly referred to as drones, are flight vehicles that can operate autonomously or be remotely controlled by a human operator or computer. Although drones were originally developed for military purposes, they have become increasingly popular in civilian applications such as logistics (see, e.g., Dayarian et al. (2020); Dorling et al. (2017); Tavana et al. (2017)); agriculture (see, e.g., Tokekar et al. (2016); Valente et al. (2013)), search and rescue (see, e.g., Miao et al. (2017); Raap et al. (2017a,b)), as well as aerial photography and surveillance (see, e.g., Cakıcı et al. (2016)).

In this paper, we consider a nested vehicle routing problem (Nested-VRP) where: (a) a single drone is deployed to survey prescribed locations; (b) the locations to be surveyed are distributed across a large geographical area; (c) the duration of the surveillance at each location is unique to the type of survey to be conducted at that location; (d) the drone has limited flight endurance; (e) a single truck with an unlimited supply of fully charged batteries is used to recharge the drone; (f) the drone must rendezvous with the truck before running out of charge; (g) the time required to swap the batteries in the drone is a prescribed positive constant; and (h) perhaps most importantly the time required to complete the sequence of surveys must be minimized.

We seek to answer the following questions: (i) What is the optimal sequence of locations for the drone to visit? (ii) At which of these locations should the drone rendezvous with the truck? and (iii) What is the optimal routing for the truck? Further, because the information must be obtained frequently and in a timely fashion, we must do so via a computationally efficient heuristic algorithm that outperforms previous algorithms.

To the best of our knowledge, we are the first to provide answers to these questions via a single formulation that incorporates the following real-world considerations: (a) non-zero surveillance times; (b) flight endurance limitations; (c) the requirement that the truck must arrive at the rendezvous location before the drone battery charge has expired; and (d) a non-zero battery swapping time. Further, we contribute to the literature on cooperative vehicle routing by:

*Corresponding author

✉ fanruiqi.zeng@gatech.edu (F. Zeng)

¹The author is affiliated with the Daniel Guggenheim School of Aerospace Engineering, Georgia Institute of Technology.

²The author is affiliated with the Department of Aerospace Engineering and Engineering Mechanics, The University of Texas at Austin.

³The author is affiliated with the H. Milton Stewart School of Industrial and Systems Engineering, Georgia Institute of Technology.

- Proposing a new Mixed Integer Programming (MIP) formulation and implementation for the vehicle routing problem.
- Analyzing and providing bounds on the compactness of our formulation.
- Investigating the complexity of the MIP model with and without prior information on the drone routing.
- Conducting extensive computational experiments from which we extract valuable insights for practitioners.

The reminder of the paper is organized as follows. In §2, we present a review of the literature on cooperative vehicle routing. Next, we describe and formulate the Nested-VRP problem in §3 followed by a discussion of model compactness and complexity. The proposed neighborhood search (NS) heuristic methodology is explained in §4, followed in §5 by a discussion of how we determine the lower bounding of its objective function value. In Section §6, we provide a detailed analysis of various numerical results as well as a case study. We share our conclusions and proposed directions for future research in §7.

2. Literature review

There continues to be growing interest in the coordinated use of drones and trucks to increase the efficiency of surveillance and transportation systems. The theoretical foundation for this work lies in the Traveling Salesman Problem (TSP) and its variant the Vehicle Routing Problem (VRP). Interested readers can consult surveys regarding solution methodologies for the TSP (see, e.g., Dantzig et al. (1954); Lin and Kernighan (1973); Rego et al. (2011)) and VRP (see, e.g., Kulkarni and Bhawe (1985); Laporte (1992); Toth and Vigo (2002)). The Nested-VRP problem we address, where we seek to optimize the routing for *a single truck and a single drone*, can be viewed as an extension of the VRP.

Several algorithms have been developed for the combined operation of a single-truck-single-drone system in a delivery context. Murray and Chu (2015) introduced the “Flying Sidekick Traveling Salesman Problem” (FSTSP), where (when appropriate) the delivery drone leaves the truck, completes a single delivery task and returns to the truck when it is at a subsequent customer location. The authors formulated the problem as a Mixed Integer Linear Program (MILP) and proposed two heuristic methodologies whose effectiveness were assessed and demonstrated via a series of computational experiments. The FSTSP heuristic starts by solving the TSP route¹ for all customers. Then, for each drone-eligible customer, the heuristic will decide whether to assign it to the drone tour or reinsert it into the truck tour at a different position in the TSP route. A similar problem, the Traveling Salesman Problem with Drone (TSP-D) was proposed by Agatz et al. (2018).

Murray and Raj (2020) subsequently extended their single-truck-single-drone framework to allow the truck to cooperate with a team of drones. Substantial time savings are achieved at the expense of more-complex coordination between vehicles. Numerous other extensions have been proposed since then: (a) improving the formulation of FSTSP such as Daknama and Kraus (2017); De Freitas and Penna (2018); Dell’Amico et al. (2019); Ha et al. (2018); (b) extending the concept to *m*-truck-*m*-drone scenarios such as Kitjachoenchai et al. (2019) and Sacramento et al. (2019); and (c) proposing new exact and heuristic methods such as Bouman et al. (2018); Poikonen et al. (2019); Schermer et al. (2018). However, the aforementioned work addresses the limited battery capacity issue by restricting the drone to visit only one intermediate location between leaving and returning to the truck. While this assumption is reasonable in delivery problems, it is quite restrictive in the case of drones performing surveillance tasks.

Poikonen and Golden (2020) introduced the “Mothership and Drone Routing Problem (MDRP)” which considers the routing of a mothership and a drone to visit several designated locations. In the infinite-capacity drone routing problem (MDRP-IC) setting, in contrast to the models mentioned in the last paragraph, the drone is allowed to visit multiple targets consecutively before returning to the mothership for refueling. They devised an exact branch-and-bound solution approach and proposed two greedy heuristic approaches that were demonstrated to be competitive in achieving near-optimal solutions. But the model is fundamentally different from the Nested-VRP problem. While the mothership can move freely in 2D continuous space, the route of the truck in our problem is restricted to the road network which is idealized as straight lines between all pairs of locations.

To date, the work most-similar in approach to ours is that of González-Rodríguez et al. (2020). They address the truck-drone team logistic (TDTL) problem via an MIP that generates the routes that the drone must follow to visit all the prescribed locations, and assigns rendezvous locations where the drone’s batteries are replaced from the truck.

¹The shortest tour for a person to visit a set of locations

Their overall goal is to minimize mission makespan. To deal with the inherent computational complexity, they propose a two-step heuristic approach and demonstrate its performance by comparing it to the exact solution obtained using the Gurobi solver. TDTL departs from the general last mile delivery problem where the drone serves one location per operation. Instead, TDTL allows the drone to serve multiple locations per excursion from the truck. Each excursion involves a set of drone actions including launching from the truck, visiting multiple locations, and returning to the truck. Even though the characteristics of their problem are similar to our problem, their model cannot be adapted to the planning of a surveillance mission. In a typical surveillance mission, the drone battery is being used both when the drone travels between locations and when it executes its observation tasks. In the extreme, one can imagine that if all the observation tasks require a full battery, then the truck would be required to visit every location to refuel the drone — which reduces the surveillance problem to a TSP for the truck.

Separately, efforts have also been made to address the battery limit issue. For example, Dorling et al. (2017) derived an energy consumption model that can further be integrated into an MILP seeking to optimize routes of a fleet of drones to complete delivery tasks. Cheng et al. (2018) studied a multi-trip drone routing problem, where payload and traveling distance are accounted for in determining the drone’s energy consumption. However, they do not consider drones working in collaboration with trucks.

All the work described above motivates the development of a Nested-VRP that takes into account the observation time at each location. Moreover, the Nested-VRP should also penalize the number of recharge stops by incurring a battery swap service time for each swap operation. And, for the sake of improving vehicle safety, the Nested-VRP should also include a restriction that the truck arrives at the rendezvous location before the drone battery is depleted.

3. Problem definition

We describe the Nested-VRP problem in §3.1, the associated mathematical formulation in §3.2, and prove some important results regarding the characteristics of our model in §3.3.

3.1. Overview

In the Nested-VRP problem, a set of geographically scattered locations is given. Each of these locations has an associated observation task with a prescribed duration.

These observation tasks are completed by a *single drone* with a limited battery life supported by a *single truck* with an unlimited supply of fully charged batteries. Specifically, the Nested-VRP problem considers the routing of the drone including traveling to and making an observation at each location. We assume the drone’s battery usage is proportional to the active flight duration (i.e., the travel time between two locations plus the observation time at the second location). Due to limitations on the drone’s battery capacity, the drone and truck must periodically meet so that an almost-discharged battery can be swapped with a completely-charged battery supplied by the truck. We assume that the truck has a sufficient stock of batteries and/or the truck has some capability to recharge batteries en route. Thus, there are no constraints on the number of completely-charged batteries that are available when the truck rendezvous with the drone. The swap process may occur during segments where the truck is carrying the drone or at survey locations either before or after the drone surveys the location. Each swap operation, including collecting the drone, swapping the batteries, and re-positioning the drone for take-off, delays the mission by a predetermined amount of service time.

The objective is to minimize the total mission time needed to complete all observation tasks including time spent traveling and conducting swapping services. Note that the total time the drone spends making observations is part of the mission but cannot be minimized because it is the sum of constant values.

To aid in our exposition of the problem and in the subsequent derivation of the mathematical formulation, we introduce the concept of a *nested unit* as shown in Figure 1. In a nested unit, the truck travels from location i to location j . Meanwhile, the drone departs from i , travels to and observes locations $\{k_1, k_2, \dots, k_m\}$, and finally meets up with the truck at location j . In summary, a nested unit consists of four components that are further explained as follows.

- **Truck bridge** refers to the arc from i to j . It connects two consecutive locations where a battery swap occurs.
- **Drone path** refers to the collection of arcs that deviate from the truck bridge, and guides the drone to observe a subset of locations assigned to the nested unit. The fact that the drone speed is usually greater than the truck speed makes it possible for the drone to observe multiple locations while the truck travels from i to j .

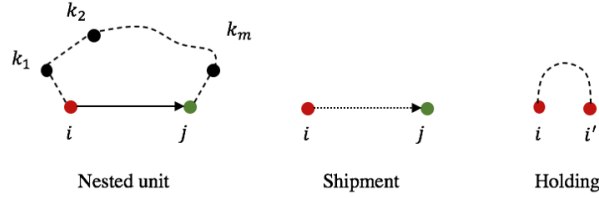


Figure 1: Illustration of a nested unit and its special formations

- Node i is a **split location** from which the drone and the truck initiate their respective next tasks (i.e., taking observations, and delivery of a new battery to the next stop). Generally, the drone gets a fully charged battery and will take off right after the swapping process. Since the truck provides the swap service, it departs no earlier than the drone.
- Node j is a **rendezvous location** at which the drone path and truck bridge merge together. A battery swap happens right after the two vehicles meet.
- In special cases, the nested unit will be transformed and reduced to a **shipment** or **holding** pattern.
 1. A **shipment** pattern occurs when the truck and the drone both decide to traverse a relatively long arc without any observation task involved during the move. We assume that when a shipment happens, the truck ships the drone and executes a battery swap while traveling along the arc without incurring extra battery swap service time.
 2. A **holding** pattern can occur at a location due to a relatively long observation period. In this case, the truck is held at the location and provides batteries to the drone both before and after the drone observes that location. In this case, the truck bridge degrades to a trivial point.

The Nested-VRP solution can be viewed as a collection of nested units without overlapping tasks. If the drone has unlimited battery capacity (i.e., infinite endurance time), the optimal solution is that the drone gets a battery at a depot once, follows a TSP route to visit and observe all locations, and returns to the depot without additional swaps along the tour. Referring to Figure 1, the optimal solution is a single large nested unit with a split location (the originating depot), a rendezvous location (the depot), and a single drone path (the TSP route). In this case, no truck bridge would be involved.

However, if the drone has limited battery capacity, the drone can only operate over relatively short time intervals without a battery swap. It follows then that the single large nested unit must be decomposed into a sequence of smaller nested units in which excessively long arcs and prolonged observation tasks will be accommodated into shipment and holding patterns, respectively. Most importantly, in each nested unit, the drone should be able to complete the specified travel and observation tasks using only its battery capacity. Therefore, the total mission is reduced to having the drone complete the relatively few tasks associated with each nested unit with battery swaps undertaken at the split and rendezvous locations.

We further require that the truck should always arrive before the drone's battery is depleted. This restriction is referred to as a **synchronization constraint**. However, there is no preference regarding the order in which the two vehicles arrive at a rendezvous location as long as the truck arrives before the drone battery charge has expired. Note that the drone may occasionally have to hover at the rendezvous location if it arrives before the truck.

To keep track of mission makespan, we define the interval between rendezvous (IBR) for each nested unit as the greater of the two vehicles' travel durations from the split location at the beginning of the nested unit to the rendezvous location at the end of the nested unit. Therefore, minimizing the mission makespan is equivalent to minimizing the summation of all the IBRs associated with nested units together with the total service times needed for battery swaps. Note that we regard a shipment as a special form of a nested unit whose IBR is the truck's travel time from one location to the next, in which case the mission makespan increases only by that amount. In that case, a battery swap may happen en route but does not delay the mission at all; and thus, the service time for a battery swap is omitted. In

the case where a nested unit reduces to a holding pattern, the truck remains stationary while the drone is observing a location. Therefore, the mission makespan increases by the amount of the drone's observation time at that location. The time increment is the IBR of the holding pattern.

3.2. Mathematical model

Given the comprehensive list of notations in Table 1, consider an undirected graph $\mathcal{G} = (\mathcal{H}, \mathcal{A})$, where $\mathcal{H} = \{0, 1, 2, \dots, n+1\}$ is the set of locations, and $\mathcal{A} = \{(i, j) \mid i \in \mathcal{H} \setminus \{n+1\}, j \in \mathcal{H} \setminus \{0\}, i \neq j\}$ is the set of arcs. Location 0 is the origin, and location $n+1$ is the eventual destination, which we force to be the origin (so that the trip starts and stops at the same place). For each location $i \in \mathcal{H} \setminus \{0, n+1\}$, let o_i be its non-negative observation time, which is assumed to be smaller than T_{bl} . If o_i were to be greater than T_{bl} , then location i must be set as a swap stop, where at least one battery swap is required (depending on the observation time); and the "final" observation time (i.e., after the last swap) is the remainder of the quotient o_i/T_{bl} , that is, $o_i/T_{bl} - \lfloor o_i/T_{bl} \rfloor$, where $\lfloor \cdot \rfloor$ denotes the "floor" function.

Table 1: Notations used in the Nested-VRP MIP formulation.

Parameters	
T_{bl}	Battery capacity of drone.
T_s	Service time needed to swap a battery.
V_D	Cruise speed of drone.
V_T	Ground traveling speed of truck.
\mathcal{H}	Set of locations in graph $\mathcal{G} = (\mathcal{H}, \mathcal{A})$.
\mathcal{A}	Set of undirected arcs in graph $\mathcal{G} = (\mathcal{H}, \mathcal{A})$.
\mathcal{S}	Set of arcs on the TSP route of a given graph \mathcal{G} .
$o_i, i \in \mathcal{H} \setminus \{0, n+1\}$	Observation time associated with location.
$\tau_{ij}^D, (i, j) \in \mathcal{A}$	Drone's flight time from i to j .
$\tau_{ij}^T, (i, j) \in \mathcal{A}$	Truck's travel time from i to j .
γ	Penalty coefficient, e.g., $\gamma = 10^6$.
Decision Variables	
$x_{ij} \in \{0, 1\}, (i, j) \in \mathcal{A}$	If $x_{ij} = 1$, the drone flies from i to j , 0 otherwise.
$y_{ij} \in \{0, 1\}, (i, j) \in \mathcal{A}$	If $y_{ij} = 1$, the truck travels from i to j , 0 otherwise.
$z_i^- \in \{0, 1\}, i \in \mathcal{H} \setminus \{0\}$	If $z_i^- = 1$, the drone swaps batteries before it observes location i , 0 otherwise.
$z_i^+ \in \{0, 1\}, i \in \mathcal{H} \setminus \{n+1\}$	If $z_i^+ = 1$, the drone swaps batteries after it observes location i , 0 otherwise.
Auxiliary Variables	
$z_i \in \{0, 1\}, i \in \mathcal{H}$	If $z_i = 1$, location i is selected as a battery swap stop, 0 otherwise.
$t_i^- \in [0, T_{bl}], i \in \mathcal{H} \setminus \{0\}$	Total travel and observation time from when drone departs the previous rendezvous location until it <i>arrives at</i> i .
$t_i^+ \in [0, T_{bl}], i \in \mathcal{H} \setminus \{n+1\}$	Total travel and observation time from when drone departs the previous rendezvous location until it <i>leaves</i> i .
$u_i \in [0, n+1], i \in \mathcal{H}$	Order index of location i in the solution of the drone route.
$w_{ij} \in \{0, 1\}, (i, j) \in \mathcal{A}$	If $w_{ij} = 1$, the truck ships the drone from location i to j , 0 otherwise.
$q_{ij} \in \mathcal{R}_+, (i, j) \in \mathcal{A}$	$\max\{0, u_j - u_i\}$.
$l_i^- \in \mathcal{R}_+, i \in \mathcal{H} \setminus \{0\}$	IBR of a nested unit that terminates before the drone observes location i .
$l_i^+ \in \mathcal{R}_+, i \in \mathcal{H} \setminus \{n+1\}$	IBR of a nested unit that terminates after the drone observes location i .

For each arc $(i, j) \in \mathcal{A}$, the time metrics τ_{ij}^T (τ_{ij}^D) represent the truck (drone) travel times between pairs of locations. We assume that the road segments between pairs of locations are straight lines. In addition, the ground speed of the truck and the cruising speed of the drone are assumed to be constants.

A mission consists of planning the drone route x_{ij} , $(i, j) \in \mathcal{A}$, to visit all locations and designing the truck route y_{ij} , $(i, j) \in \mathcal{A}$, to delivery fully charged batteries. Specifically, the drone route and the truck route should intersect at a subset of locations z_i , $i \in \mathcal{H}$ where the truck performs battery swaps for the drone. The primary goal is to minimize the total mission time while operational constraints are satisfied.

Next, we explain different sets of operational constraints in §§3.2.1–3.2.4. Constraints from the same set serve a particular function. In §3.2.5, we put together all of the constraints and present the full Nested-VRP formulation.

3.2.1. Drone route construction

The drone departs from location 0 and eventually returns to location $n + 1$. To ensure each location is observed exactly once, we require that every location in $\mathcal{H} \setminus \{0, n + 1\}$ has one incoming arc and one outgoing arc. Therefore, we have the following set of constraints:

$$\sum_{j:(i,j) \in \mathcal{A}} x_{ij} = 1, \quad \forall i \in \mathcal{H} \setminus \{n + 1\} \quad (1)$$

$$\sum_{i:(i,j) \in \mathcal{A}} x_{ij} = 1, \quad \forall j \in \mathcal{H} \setminus \{0\} \quad (2)$$

The above constraints are not sufficient to construct the tour because they are also satisfied by subtours in the graph. We further introduce auxiliary variables u_i , $i \in \mathcal{H}$, which indicate the order of locations along the drone route. Any potential subtours in the graph will be eliminated by enforcing the following constraints: (Miller et al., 1960).

$$u_0 = 0 \quad (3)$$

$$1 \leq u_i \leq n + 1, \quad \forall i \in \mathcal{H} \setminus \{0\} \quad (4)$$

$$u_i - u_j + 1 \leq (n + 1)(1 - x_{ij}), \quad \forall (i, j) \in \mathcal{A}, i \neq 0 \quad (5)$$

3.2.2. Truck route construction

Likewise, the truck departs from location 0 and returns to location $n + 1$ at the end of the trip. In the special case where the drone can finish the entire mission without any battery swaps, the truck parks at the origin 0. Note that the truck route is constructed in such a way that the truck only serves locations that are selected as battery swap stops (i.e., $z_i = 1$). Most importantly, the truck visits the swap locations in the same order as that of the drone. The above requirements are captured by the following constraints:

$$\sum_{j:(0,j) \in \mathcal{A}} y_{0,j} \leq 1; \quad \sum_{i:(i,n+1) \in \mathcal{A}} y_{i,n+1} \leq 1 \quad (6)$$

$$\sum_{i:(i,j) \in \mathcal{A}} y_{ij} = z_j; \quad \sum_{k:(j,k) \in \mathcal{A}} y_{jk} = z_j, \quad \forall j \in \mathcal{H} \setminus \{0, n + 1\} \quad (7)$$

$$y_{ij} \leq \max\{0, u_j - u_i\}, \quad \forall (i, j) \in \mathcal{A} \quad (\star)$$

Observe that in constraint (\star) , the quantity $\max\{0, u_j - u_i\}$ can be represented by the solution to the following optimization problem.

$$\min\{q_{ij} : q_{ij} \geq 0, q_{ij} \geq u_j - u_i\} \quad (8)$$

Since the Nested-VRP problem (defined formally in §3.2.5) is also a minimization problem, we can add $\gamma \sum_{(i,j) \in \mathcal{A}} q_{ij}$ to the objective function, where γ is a large-enough (penalty) constant. This allows us to rewrite the constraint (\star) as follows.

$$y_{ij} \leq q_{ij}, \quad q_{ij} \geq u_j - u_i, \quad q_{ij} \geq 0, \quad \forall (i, j) \in \mathcal{A} \quad (9)$$

To ensure the synchronization constraint, the truck must spend no more than T_{bl} time in transit between two con-

secutive rendezvous locations. This can be captured by the following constraint in which $M_1 = \sum_{(i,j) \in \mathcal{A}} \tau_{ij}^T$.

$$\tau_{ij}^T y_{ij} \leq T_{bl} + M_1 w_{ij}, \quad \forall (i, j) \in \mathcal{A} \quad (10)$$

In the special case where the truck ships the drone (i.e., $w_{ij} = 1$), the synchronization constraint becomes redundant.

3.2.3. Time flow balance

To keep track of the drone's battery consumption, we create an artificial timer. The timer records the current battery consumption of the drone by accumulating the total travel and observation time since leaving the previous rendezvous location. At each location, we introduce auxiliary variables $t_i^-, t_i^+ \in [0, T_{bl}]$, which we refer to as the state of timer at location i . In particular, t_i^- denotes the state of the timer when the drone arrives at location i and t_i^+ denotes the state of the timer when the drone is about to leave location i . Once a timer is about to exceed the battery capacity T_{bl} , the timer is reset to 0, corresponding to a battery swap.

Constraint (11) describes the change of the states of the timer due to an observation task at location i . When the drone arrives at location i , if the drone does not have sufficient battery time to continue and observe location i , we designate i as a rendezvous location for battery replacement (i.e., $z_i^- = 1$). When the drone is about to leave location i , the total travel and surveillance time t_i^+ from when the drone departs the previous rendezvous location until it leaves location i is only the observation time o_i . However, if the drone has enough battery time to continue observing location i at arrival (i.e., $z_i^- = 0$), the timer keeps accumulating the drone flight time and increases by the amount o_i . In this case, when the drone leaves location i , the state of the timer t_i^+ becomes $t_i^- + o_i$.

Constraints (12)–(18) describe the change of states of the timer due to the drone travel from one location to the other. The battery consumption on any arc $(i, j) \in \mathcal{A}$ depends on both the drone route decision x_{ij} and the truck shipment decision w_{ij} associated with the arc (i, j) . Constraints (12)–(14) ensure that the truck ships the drone (i.e., $w_{ij} = 1$) if the two vehicles have decided to traverse the same arc (i, j) .

Typically, the drone travels from location i to location j alone, i.e., $x_{ij} = 1$ and $w_{ij} = 0$. Recall that the timer state is t_i^+ when the drone is about to leave location i and t_j^- when the drone arrives at location j . According to constraints (15)–(18), if arc (i, j) is activated as part of the drone route, the states of the timer at both sides of the arc (i, j) are regulated by the equation $t_j^- = t_i^+(1 - z_i^+) + \tau_{ij}^D$. Specifically, if the drone has sufficient battery to cover the arc (i, j) , the drone requires no additional battery swaps (i.e., $z_i^+ = 0$) before leaving i . Therefore, the timer increases by the amount of traveling time τ_{ij}^D , and t_j^- becomes $t_i^+ + \tau_{ij}^D$ when the drone arrives at location j . However, if the drone requires a battery swap to be able to cover arc (i, j) , a rendezvous location is added when the drone departs location i (i.e., $z_i^+ = 1$). In this case, since the timer is set to 0 at the beginning of the arc traveling, the timer accumulates the amount of the drone traveling time and becomes τ_{ij}^D when the drone reaches the endpoint of arc (i, j) .

In the special case in which the truck ships the drone from location i to location j (i.e., $w_{ij} = 1$ and $x_{ij} = 1$), a rendezvous location at i has to be created (i.e., $z_i^+ = 1$) so that the truck can pick up the drone. Constraints (15)–(18) regulate the states of the timer at both sides of arc (i, j) . When the shipment happens, no matter what state the timer is just before the drone leaves location i , the timer is set to T_{bl} at the time the drone arrives at location j . Given that $t_j^- = T_{bl}$, constraint (11) ensures that a rendezvous location is placed at j (i.e., $z_j^- = 1$). By doing so, the drone continues the mission with a new battery after it arrives at location j . Note that the truck does not perform battery swaps at the rendezvous locations placed at both endpoints of the arc (i, j) . Therefore, these two rendezvous locations do not delay the mission (see objective function (25)).

Arc (i, j) has no impact to the state of the timer if it is not part of the drone route. This can be captured by constraints (15)–(16) in which $M_2 = T_{bl}$. In Figure 2, we illustrate how the state of the timer is updated as the mission continues.

$$t_i^+ = t_i^-(1 - z_i^-) + o_i, \quad \forall i \in \mathcal{H} \setminus \{n+1\} \quad (11)$$

$$w_{ij} \leq x_{ij}, \quad \forall (i, j) \in \mathcal{A} \quad (12)$$

$$w_{ij} \leq y_{ij}, \quad \forall (i, j) \in \mathcal{A} \quad (13)$$

$$x_{ij} + y_{ij} \leq 2w_{ij}, \quad \forall (i, j) \in \mathcal{A} \quad (14)$$

$$t_j^- \leq t_i^+(1 - z_i^+) + \tau_{ij}^D + (T_{bl} - \tau_{ij}^D)w_{ij} + M_2(1 - x_{ij}), \quad \forall (i, j) \in \mathcal{A} \quad (15)$$

$$t_j^- \geq t_i^+(1 - z_i^+) + \tau_{ij}^D + (T_{bl} - \tau_{ij}^D)w_{ij} - M_2(1 - x_{ij}), \quad \forall (i, j) \in \mathcal{A} \quad (16)$$

$$t_j^- \leq T_{bl}, \quad \forall j \in \mathcal{H} \setminus \{0\} \quad (17)$$

$$t_j^+ \leq T_{bl}, \quad \forall j \in \mathcal{H} \setminus \{n+1\} \quad (18)$$

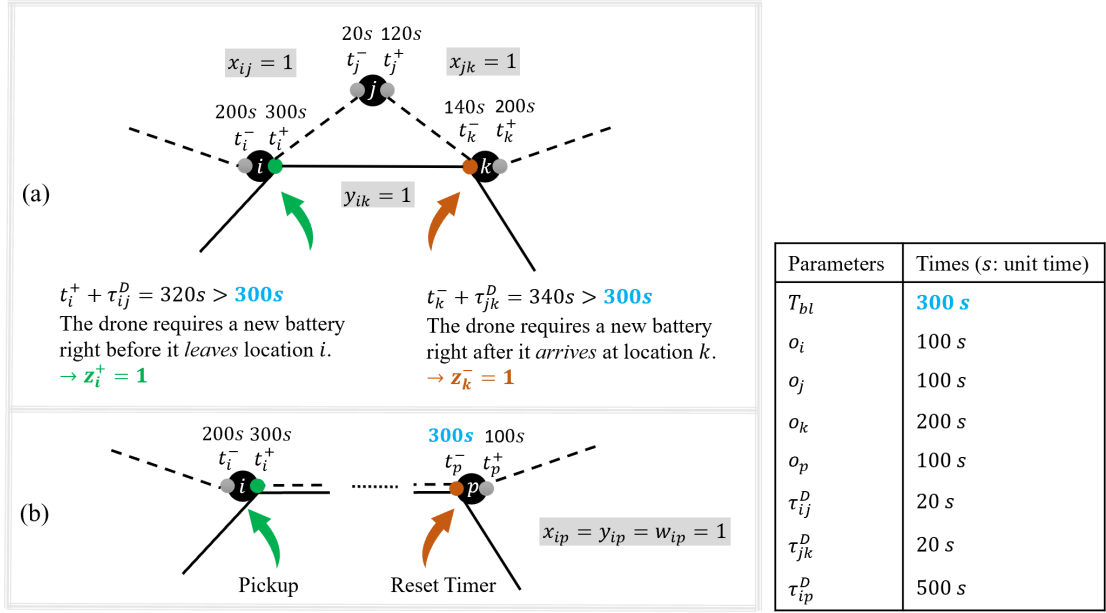


Figure 2: Time flow balance example. (a) Typically, a battery swap can occur when the drone is about to leave a location (green dot) or when it just arrives at a location (red dot). (b) In the special case where the truck ships the drone, a rendezvous location, corresponding to a pickup, is placed before they start traveling (green dot). A rendezvous location is also placed at the end of travel (red dot). Notice that the timer is manually adjusted to T_{bl} when the two vehicles arrive at the designated location p .

3.2.4. Interval between rendezvous

With the help of the timer from the previous section, we now derive the IBR for each nested unit. Notice that for a location that is not a battery swap stop, the IBR of such a location is trivial as stated in constraints (19)–(20). A nested unit can only terminate at rendezvous location j either before or after the drone observes the location j .

Let l_j^- denote the IBR for the nested unit that terminates when the drone arrives at location j . IBR l_j^- is determined by comparing the truck's travel time $\sum_{i:(i,j) \in \mathcal{A}} \tau_{ij}^T y_{ij}$ and the drone's surveillance time $t_j^- - T_{bl} \sum_{i:(i,j) \in \mathcal{A}} w_{ij}$ since they both leave the previous rendezvous location. In the special case when the nested unit is a shipment pattern (i.e., $\sum_{i:(i,j) \in \mathcal{A}} w_{ij} = 1$), the drone timer t_j^- at location j becomes T_{bl} due to constraints (15)–(16). In this case, the drone's surveillance time becomes trivial, and thus the IBR l_j^- becomes equal to the truck's travel time $\sum_{i:(i,j) \in \mathcal{A}} \tau_{ij}^T y_{ij}$.

Likewise, let l_j^+ denote the IBR for the nested unit that ends after the drone observes location j . IBR l_j^+ is the maximum of the truck's travel time $\sum_{i:(i,j) \in \mathcal{A}} \tau_{ij}^T y_{ij} (1 - z_j^-)$ and the drone's surveillance time t_j^+ for the nested unit. Notably, if the nested unit reduces to a holding pattern (i.e., $z_j^- = z_j^+ = 1$), then the truck's travel time becomes 0, and thus IBR l_j^+ should be equal to the drone's surveillance time t_j^+ .

As a summary, the following constraints (21)–(24) are necessary to define IBRs for all possible swap locations.

$$l_j^- \leq z_j T_{bl}, \quad \forall j \in \mathcal{H} \quad (19)$$

$$l_j^+ \leq z_j T_{bl}, \quad \forall j \in \mathcal{H} \quad (20)$$

$$l_j^- \geq t_j^- - T_{bl} \sum_{i:(i,j) \in \mathcal{A}} w_{ij} - M_2(1 - z_j^-), \quad \forall j \in \mathcal{H} \quad (21)$$

$$l_j^- \geq \sum_{i:(i,j) \in \mathcal{A}} \tau_{ij}^T y_{ij} - M_1(1 - z_j^-), \quad \forall j \in \mathcal{H} \quad (22)$$

$$l_j^+ \geq t_j^+ - M_2(1 - z_j^+), \quad \forall j \in \mathcal{H} \quad (23)$$

$$l_j^+ \geq \sum_{i:(i,j) \in \mathcal{A}} \tau_{ij}^T y_{ij}(1 - z_j^-) - M_1(1 - z_j^+), \quad \forall j \in \mathcal{H} \quad (24)$$

3.2.5. Overall formulation

Our objective is to minimize the mission makespan, which consists of the drone surveillance time and the total service time for battery swaps—except when the truck ships the drone from location i to j , in which case the battery swap that happens en route does not delay the mission. Moreover, the quantity $\gamma \sum_{(i,j) \in \mathcal{A}} q_{ij}$ as discussed in §3.2.2 is added to the objective function. To initialize the mission, we assume that the drone is equipped with a new battery before leaving origin 0, so that $z_0^+ = 1$ and $t_0^+ = 0$. The complete Nested-VRP model is given as follows.

$$\begin{aligned} (\text{Nested-VRP}) \quad \min \quad & \sum_{i \in \mathcal{H}} (l_i^- + l_i^+) + T_s \sum_{i \in \mathcal{H}} \left(z_i^- + z_i^+ - \sum_{j:(i,j) \in \mathcal{A}} 2w_{ij} \right) + \gamma \sum_{(i,j) \in \mathcal{A}} q_{ij} \\ \text{s.t.} \quad & \text{constraints (1)–(24)} \\ & z_0^+ = 1, \quad t_0^+ = 0 \\ & x_{ij} \in \{0, 1\}, \quad y_{ij} \in \{0, 1\}, \quad w_{ij} \in \{0, 1\}, \quad q_{ij} \in \mathcal{R}_+, \quad \forall (i, j) \in \mathcal{A} \\ & z_i^-, z_i^+, z_i \in \{0, 1\}, \quad u_i \in [0, n+1], \quad t_i^-, t_i^+ \in \mathcal{R}_+, \quad l_i^-, l_i^+ \in \mathcal{R}_+, \quad \forall i \in \mathcal{H} \end{aligned} \quad (25)$$

3.3. Model characteristics

In §3.3.1, we compare the Nested-VRP model to what we regard as the state-of-the-art model in terms of their relaxed polyhedra. Next, in §3.3.2, we investigate the complexity of the Nested-VRP model given prior drone route information.

3.3.1. Relationship to the state-of-the-art model

From a modeling perspective, it is of particular interest to compare the compactness of the proposed MIP model to other state-of-the-art models. To the best of our knowledge, the most-similar model concerning truck-drone coordinated routing is that of González-Rodríguez et al. (2020) — the Truck Drone Team Logistics (TDTL) model. Since the TDTL model does not consider the observation times associated with each location nor the service time in swapping the battery, we will first derive a special version of the Nested-VRP model where we neglect the battery swap service time and set the observation time to zero for every location. Our special version of the Nested-VRP is called Zero Observation Nested-VRP (ZONVRP). Since the two models to be compared apply different notations with different physical meanings, a linear transformation Φ that maps the ZONVRP variables to that of TDTL is needed. We will show that the linear programming (LP) relaxation of the Nested-VRP model is tighter than the LP relaxation of the TDTL with respect to a linear transformation. This is noteworthy because the majority of commercial MIP solvers have a branch-and-bound component that leverages the associated LP to iteratively search for the optimal solution. Thus, a tighter formulation usually requires the evaluation of fewer branching nodes thereby reducing computation time. Further, even if the optimal solution can not be obtained within the time limit, the MIP solver can provide a better bound on the optimal value of the problem at termination when using a tighter formulation.

Theorem 1. *Denote the feasible set of ZONVRP under a linear transformation Φ as P_1 , and denote the feasible set of TDTL as P_2 . Then P_1 is a proper subset of P_2 . (See Appendix A for Φ construction and a detailed proof.)*

3.3.2. Model complexity

To understand the complexity of the Nested-VRP model, we will evaluate the computational effort required throughout the decision-making process. (I) First, the drone route is constructed by sequencing n locations. Together with the origin 0 and eventual destination $n+1$, there exists $n!$ different drone routes. Each possible drone route has a unique battery consumption pattern along the tour. (II) Second, given a specific possible drone route, the swap stops assignment is a problem of finding a subset of locations that naturally split the drone route into path segments. In particular, the drone's flight duration and the truck's ground travel time for each of these segments should both be within the battery limit. We can see that the choices of the set of charging locations is highly sensitive to the battery usage corresponding

to the drone route. Thus, if implementing a drone route requires excessive battery swaps to ensure flight continuity, an adjustment to the drone route may reduce the coordination effort for the truck to serve batteries. As the name of the model suggests, the decisions regarding the drone route and truck route are intertwined dynamically and tied by the decisions on swap locations. To solve the Nested-VRP problem, we should navigate through the tasks of planning a good drone route and scheduling battery swaps in a versatile manner. Neither component seems to dominate the other, and that question merits further investigation—if partial information about the Nested-VRP solution is given, how much effort is needed to obtain the complete Nested-VRP solution?

In the following, we will demonstrate that, given a fixed order for the drone to visit all locations, we can solve within polynomial time the remaining Nested-VRP solution—including the truck route and the placement of swap stops—that minimizes the mission makespan.

Theorem 2. *Given a fixed order of a set of locations representing a known drone route, the partial Nested-VRP solution—including a subset of locations as swap stops and the truck route—can be solved in polynomial time.*

PROOF. With the drone route specified, the optimal Nested-VRP solution can be obtained by finding the cheapest collection of non-overlapping nested units such that the union of the drone paths from each unit aligns with the predetermined drone route. In the following, we will first construct the set of all feasible nested units. Each of these nested units is associated with a cost (i.e., IBR). Then, the collection of nested units (CNU) with the smallest mission time is obtained by solving an integer program efficiently. We name it the CNU problem.

Let $(s_0, s_1, \dots, s_{n+1})$ be a permutation of the node set \mathcal{H} , where $s_0 = 0$ and $s_{n+1} = n + 1$. In following this order, the drone departs from a location s_i , travels to the next location s_{i+1} which takes time $\tau_{s_i s_{i+1}}^D$, and spends $o_{s_{i+1}}$ time for surveying location s_{i+1} . Let $W = (w_1, w_2, \dots, w_{2n+1})$ denote the consecutive tasks to be completed by the drone in the mission, where $w_1 = \tau_{s_0 s_1}^D, w_{2k} = o_{s_k}, w_{2k+1} = \tau_{s_k s_{k+1}}^D, \forall k = 1, \dots, n$. Without loss of generality, we assume that a rendezvous location is placed at the beginning of the mission which corresponds to equipping the drone with a full battery. In addition, for simplicity, we assume that any other rendezvous location $i \in \{1, \dots, 2n+1\}$ should be limited to where the task w_i is completed (i.e., the drone just arrives at a location or just completes an observation task).

For a nested unit with the first rendezvous location at the end of completing task w_i and the second rendezvous location at the end of completing task w_j , we denote the nested unit as $(i, j, l_{ij}), i, j \in \{1, \dots, 2n+1\}, i < j$, where l_{ij} is the interval between rendezvous of the unit. To determine l_{ij} , we further define $D_{ij} = \sum_{k=i+1}^j w_k$ as the total drone travel and surveillance time for completing the $(i+1)$ th task and all others up to and including the j th task. Likewise, define T_{ij} as the truck travel time moving from where the i task is completed to where the j th task will be completed by the drone. A nested unit is feasible if both D_{ij} and T_{ij} are within the battery limit T_{bl} . The nested unit, if picked, will delay the mission by $l_{ij} \in \mathcal{R}_+$, which is defined as follows.

$$l_{ij} = \begin{cases} \infty & \text{if } D_{ij} \geq T_{bl} \text{ or } T_{ij} \geq T_{bl} \\ \max(D_{ij}, T_{ij}) & \text{otherwise} \end{cases}$$

Let $U = \{(i, j, l_{ij}) : \forall i, j \in \{1, \dots, 2n+1\}, i < j\}$ denote the set of all possible formations of nested units, the CNU problem is to find the least-delayed subset of nested units such that all tasks are completed/covered exactly once.

We now formulate the CNU problem. Define the binary matrix $A \in \{0, 1\}^{|U| \times |W|}$. For each nested unit $u \in U$, we have $A_{uk} = 1$ if task w_k is covered by nested unit u , and 0 otherwise. For simplicity, let l_u represents the time cost of nested unit u . Define decision variables $x_u = \{0, 1\}, \forall u \in \{1, \dots, |U|\}$. If $x_u = 1$, then nested unit u is selected, 0 otherwise.

$$\begin{aligned} \text{(CNU)} \quad \min \quad & \sum_{u=1}^{|U|} l_u x_u + T_s \sum_{u=1}^{|U|} x_u \\ \text{s.t.} \quad & \sum_{u=1}^{|U|} A_{uk} x_u = 1, \quad \forall k \in \{1, 2, \dots, 2n+1\} \\ & x_u \in \{0, 1\}, \quad \forall u \in \{1, 2, \dots, |U|\} \end{aligned} \tag{26}$$

The matrix A is total unimodular (TU) since each row of matrix A consists of consecutive ones (Schrijver, 1998). Then since A is TU, the non-empty polyhedron $P(b) = \{Ax = b, x \geq 0\}$ is integral for the all-integral vector b

(Nemhauser and Wolsey, 1999); in our case, b is a vector of all 1s. Therefore, we can solve the CNU model by solving its linear relaxation and still achieve integer solutions. The time effort in solving a linear program is polynomially bounded by the total number of variables $|U|$ (Karmarkar, 1984).

4. Heuristic methodology via neighborhood search

The nested-VRP problem, being an extension of the Traveling Salesman Problem, is difficult from a theoretical perspective. In particular, as the size of the problem increases, the complexity of the MIP model and limited computation time do not allow for an exact solution. This motivates us to develop a heuristic methodology that is expected to produce good solutions given a computational time budget.

The neighborhood search (NS) framework, first introduced in Shaw (1998), has been demonstrated as a powerful tool for solving difficult combinatorial optimization problems. A generic NS starts with an initial feasible solution to the problem of interest. Each NS iteration involves destructing the current best-known solution and reconstructing a better candidate by modifying local decisions. The best solution obtained by the time of termination is recorded as the final result.

As we have discussed, the optimal Nested-VRP solution can be characterized as the time-minimizing collection of non-overlapping nested units each of which obeys the battery capacity limit and the synchronization constraint. Given a Nested-VRP instance, we denote its optimal solution as I_{opt} which consists of the optimal configuration of nested units. In our NS framework, we start with a feasible solution I of the same instance. Initially, the feasible solution I forms the nested units in a suboptimal way (i.e., at least one nested unit does not match that in the optimal solution sol). Next, I can be further improved by iteratively destructing mismatched nested units and regrouping them with their neighboring units. When the search process terminates, the heuristic returns the best known solution I^* . Therefore, the key to success of an NS heuristic approach to solving the nested-VRP problem boils down to: (i) Finding a good initial feasible solution that contains the least possible mismatched nested units in comparison to the true (unknown) optimal solution as a starting point. (ii) Identifying the set of undesirable nested units that are more likely mismatched compared to the (unknown) optimal solution. (iii) An effective destruction and reconstruction process to fix the local mismatches.

We summarize the overall NS heuristic in Figure 3. The initialization, destruction, reconstruction, and termination components are further discussed in §§4.1, 4.2, 4.3, and 4.4, respectively. In addition, a formal description of the NS heuristic is stated at the end of this section.

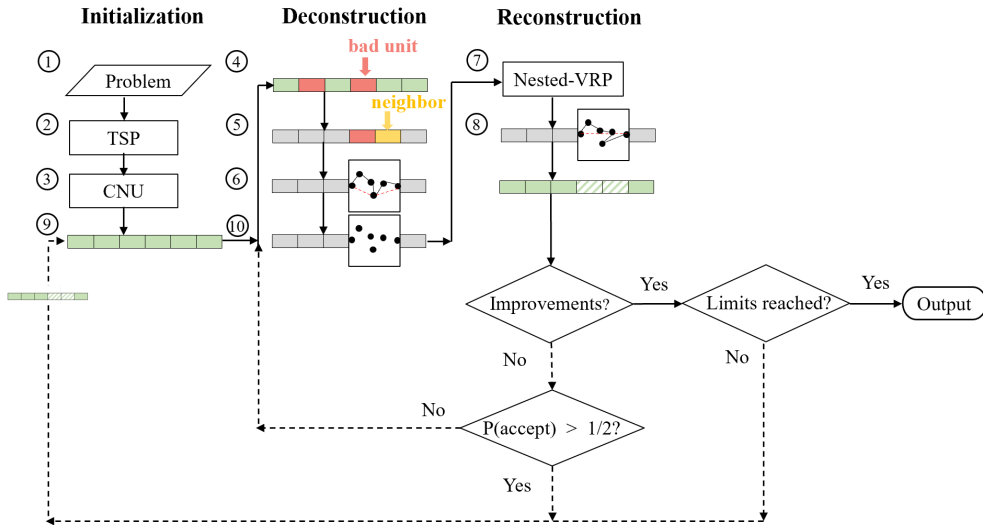


Figure 3: Flow chart for the NS heuristic, including Initialization, Destruction, and Reconstruction phases.

4.1. Initialization

Suppose that the order to visit all locations (i.e., the drone route) is given. By Theorem 2, the full set of Nested-VRP solutions can be determined by further solving the CNU problem (26). Therefore, finding a good initial drone route is critical in obtaining a feasible Nested-VRP solution.

We expect that the initial feasible solution has as few mismatched nested units compared to the unknown optimal solution. Empirically, we have observed from the solutions of small-size problems (whose exact optimal solutions are actually obtainable) that even if the TSP order is not always guaranteed to be the best drone route, it at least aligns with the optimal drone routing most of the time. In fact, in the situation where the true optimal drone route is not the TSP route, we have still empirically observed that a large portion of nested units, both in the heuristic solution and the optimal solution, share the same configurations.

Thus, in the initial Nested-VRP solution, we enforce that the drone route is the same as the TSP route, i.e., the shortest-time tour to visit every location exactly once. With the known drone route, the decisions on the truck route and the assignment of battery stops along the tour can be obtained by further solving the CNU problem (see Figure 3, steps 1–3).

4.2. Destruction

Given a feasible solution to be improved, the destruction process is to remove the nested units that are likely misaligned with those in the true optimal solution. Since the Nested-VRP problem favors a solution with a minimum makespan, each nested unit is expected to pack in as many observation tasks and be as efficient with battery energy as possible. Therefore, if one nested unit only consumes a small fraction of battery capacity and leaves a great amount of energy wasted when a new battery swap occurs, the nested unit is identified as undesirable. This fraction is set as a user-defined threshold of $\beta \in [0, 1]$. A nested unit u is deemed to be a bad unit if the amount of wasted battery capacity, named battery slackness δ_u , exceeds βT_{bl} .

With bad nested units identified, the NS heuristic proceeds to destroy the bad nested unit itself as well as its neighbors. Regarding the severity of the destruction process, if the impacted neighborhood is limited, there is not much freedom for the reconstruction process to identify a better choice. On the contrary, once a large portion of the initial solution is destroyed, the reconstruction process is equivalent to resolving a Nested-VRP of a relatively larger size. To alleviate the brunt of computational complexity per iteration, we currently restrict the destruction process to the bad unit plus a single neighbor located either immediately before or after the bad unit. At the end of the destruction process (see Figure 3, steps 4–6), we obtain a set of locations that were previously covered by the bad unit and its neighbor. To complete the observation tasks at these locations, we still need to determine the drone route, truck route, and assignment of the battery swap stops for coordinating the truck and the drone. We present the destruction function in Algorithm 1.

Algorithm 1: Destruction Function

Data: I : The best-known solution;
Result: U : bad nested units to be destroyed;
 L : the set of locations that are included in set U ;
 $pool = \emptyset$;
 $U = \emptyset$;
 $L = \emptyset$;
for nested unit u in I **do**
 if $\delta_u \geq \beta T_{bl}$;
 $pool \leftarrow pool \cup \{\text{nested unit } u\}$;
end
 $U \leftarrow$ randomly choose a unit from $pool$ and pick one of its neighboring units ;
 $L \leftarrow$ locations that are covered by nested units in U ;

4.3. Reconstruction

Nested units that have been destroyed at the end of the destruction process are in the form of free locations in the graph. In the reconstruction process, our goal is to sequence the free locations and pick a subset of the free locations as swap stops to minimize the total time for the drone to receive battery replacements, travel, and complete observation

tasks associated with these free locations. This can be carried out by solving the Nested-VRP model on the free locations locally and exactly.

Even though the Nested-VRP model suffers from computational complexity as the size of the problem increases, in the reconstruction process, the number of locations that need to be solved in each iteration is relatively small. This enables us to take advantage of the Nested-VRP MIP model that produces a local operation plan with the smallest makespan (see Figure 3, steps 7–8). Interestingly, during the local reconstruction, the order of the free locations will be altered to explore the portion of time-saving benefits lost due to pre-fixing the drone route.

At the end of the reconstruction process, we obtain a new set of nested units. Compared to the grouping before being destructed, if the new sets have a smaller makespan, we accept the solution and replace the old grouping with the new one (see Figure 3, step 9). Otherwise, we will accept it with a probability $1/2$. Accepting a worse solution allows the heuristic to step out of a local minimum and explore for the global minimum. If the solution is rejected, the heuristic proceeds to the next iteration with the same best-known solution (Figure 3, step 10). After that, the destruction process picks a different bad unit and continues the search process. The reconstruction function is detailed in Algorithm 2.

Algorithm 2: Reconstruction Function

Data: I : The best-known solution;
 U : The set of bad units;
 L : The set of locations that are covered by bad units;
Result: I' : a candidate solution;
 $L' = \text{Nested-VRP}(L)$; // L' is a collection of nested units obtained by solving the Nested-VRP model on locations in L
 $I' \leftarrow (I \setminus U) \cup L'$; // merge good nested units with the newly formed nested units

4.4. Termination criteria

The destruction and reconstruction process is repeated until the makespan savings between iterations become marginal. Specifically, if there is no improvement achieved for K consecutive iterations, then the loop is terminated. Also, to safeguard the run-times, we restrict the total number of iterations to N_{\max} , which is instance dependent.

As a reflection, the art of performing this heuristic involves starting with a good feasible solution, exploring possible nested units for potential improvements, and optimizing Nested-VRP exactly on a local scale. At a higher level, the iterations between destruction and reconstruction can be viewed as a negotiation between the drone and truck routing decisions. Given a drone route, the truck can accept part of the workload for good nested units and reject the leftover workload required by bad nested units. In return, the drone will change its route with the hope that both parties are satisfied. The overall heuristic methodology is formally stated in Algorithm 3.

Algorithm 3: NS Heuristic Overview

Data: Nested-VRP Problem;
Result: I^* : the best known collection of nested units;
 $S = \text{TSP}(\text{Problem})$;
 $I = \text{CNU}(S)$;
while *Stopping condition is not satisfied* **do**
 $U, L = \text{Destruction}(I)$;
 $L' = \text{Nested-VRP}(L)$;
 $I' = \text{Reconstruction}(I \setminus U, L')$;
 if I' shows improvement **then**
 $I \leftarrow I'$;
 Update stopping criteria;
 else
 $I \leftarrow I'$ with probability $1/2$;
 Update stopping criteria;
 end
end
return $I^* = I$

5. Lower bounding method

For an optimization problem, a lower bound is a value that is known to be less than or equal to the optimum. Generally, a lower bound is used for evaluating the quality of a solution solved by a heuristic when the optimal solution is unattainable. Ideally, a tighter lower bound gives a more-qualified guarantee of a near-optimal solution. In this section, we focus on deriving a lower bound on the mission makespan of the Nested-VRP problem. We compare the solutions obtained by the NS heuristic to the lower bound value. The tightness of the proposed lower bound will be evaluated in future work.

We start by investigating the battery usage in each of the nested units in the solution. Given a nested unit u , the drone surveillance time includes time spent on traveling between locations and completing observing tasks. As depicted in Figure 4(a), if the truck arrives at a rendezvous location first, then once the drone arrives at the rendezvous location, the drone relinquishes all remaining battery life before it obtains a new battery. The battery slackness is denoted as δ_u . However, in Figure 4(b), if the drone arrives at the rendezvous location first, the drone will idle for time Δ_u while waiting for the truck. Once the truck arrives, the drone lands on the truck and releases all remaining battery life δ_u .

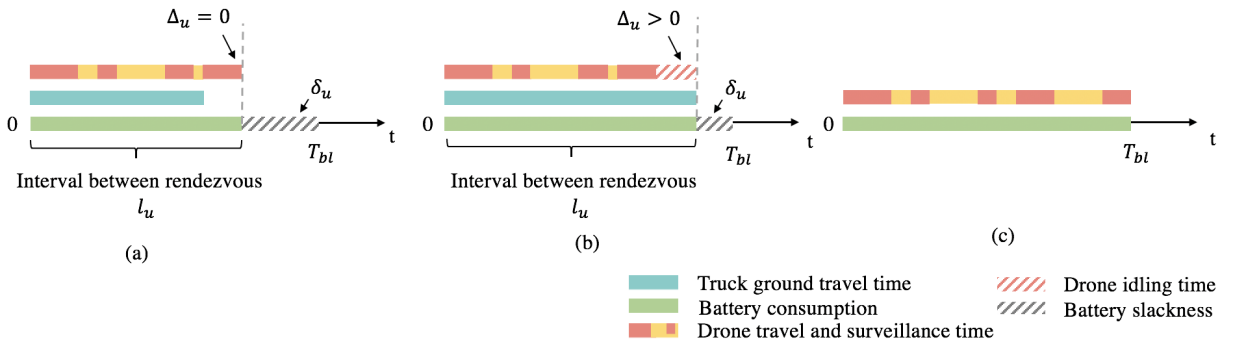


Figure 4: Battery usage in a nested unit. (a) The drone arrives later than the truck and thus the IBR l_u of the nested unit is determined by the drone's surveillance time (i.e., traveling and observing). The drone's idling time Δ_u is 0. The wasted battery energy δ_u is the difference between T_{bl} and l_u . (b) The truck arrives later than the drone and thus the IBR l_u of the nested unit is determined by the truck's traveling time. The drone arrives at the rendezvous location and idles for time Δ_u . The wasted battery energy δ_u is the difference between T_{bl} and l_u . (c) The drone battery can be swapped at anytime, anywhere. Thus, the drone's idling time δ_u and the wasted battery time $T_{bl} - l_u$ are trivial.

A lower bounding technique is based on relaxing some of the constraints in the original Nested-VRP model. First, instead of restricting the swap stops to take place at locations, the drone is allowed to replace its battery either en route from one location to the other or while observing at a location. Second, we simplify the synchronization constraint that ordinarily requires the truck to meet up the drone before the drone battery charge has expired; now we allow the drone to replace the battery itself without the truck being involved. This relaxed Nested-VRP is illustrated in Figure 4(c). In this case, the drone idling time Δ_u and battery slackness δ_u are trivial. It is clear that the total number of swap stops is purely proportional to the battery consumption that occurs only during drone travel and surveillance activities.

Given the above relaxations, an optimistic estimate of the mission makespan consists of the following three components: (i) the minimum time spent in drone routing (i.e., the TSP route); (ii) the constant time spent in observing locations; and (iii) the smallest number of swap stops multiplied by the battery swap service time. We formally establish the lower bound on the objective value of the Nested-VRP model in Theorem 3.

Theorem 3. *Given a Nested-VRP instance described in graph $\mathcal{G} = (\mathcal{H}, \mathcal{A})$, let S denote the set of arcs on the TSP route where $S = \{(i, j) : (i, j) \in \mathcal{A}, (i, j) \text{ is on the TSP route}\}$. The lower bound on the value of an optimal solution of the Nested-VRP problem, LB , can be computed by Equation (27). (See Appendix B for the detailed proof.)*

$$LB = \sum_{(i,j) \in S} \tau_{ij}^D + \sum_{k \in \mathcal{H}} o_k + \lfloor \frac{1}{T_{bl}} \left(\sum_{(i,j) \in S} \tau_{ij}^D + \sum_{k \in \mathcal{H}} o_k \right) \rfloor T_s \quad (27)$$

6. Computational experiments

6.1. Experimental setup

In this section, we conduct a series of experiments to investigate the performance of two different approaches: the MIP and the NS heuristic. Our goals are two-fold: (i) From an algorithm design standpoint, we will demonstrate that the proposed heuristic is adequate to support the drone-truck surveillance mission. (ii) From an operational standpoint, we will further examine how to achieve the most-economic solution by carefully analyzing the model parameters.

All experiments are performed on a set of benchmark instances from Agatz et al. (2018) where the authors randomly generate locations on a 2D plane following different patterns, which are labeled: uniform, single-center, and double-center. The uniform pattern consists of locations whose x and y coordinates are uniformly sampled from $\{0, \dots, 100\}$ independently. The single-center represents a circular city in which locations are closer to the center with higher probability. The double-center pattern mimics a city with two centers that are 200 distance units away from each other. Around each center, locations are distributed in the same way as the single-center pattern. The benchmark dataset is naturally split into small cases and large cases according to the number of locations, N . The “small” set considers possible location numbers $\{5, 6, 7, 8, 9, 10\}$ while the “large” set considers numbers in the pool of $\{20, 50, 75, 100, 175, 250\}$. By default, the drone’s cruising speed is 1 unit distance per unit time. By varying the truck speed among $\{1, 0.5, 0.3333\}$, while keeping the drone speed as 1, we achieve the speed ratios $\alpha = \{1, 2, 3\}$ between the two vehicles. For clarity, a scenario is referred to as a subset of data sharing the same (pattern, N , α) characteristics. One scenario includes 10 instances. For example, scenario (pattern=uniform, $N = 5$, $\alpha = 1$) consists of 10 instances, where each instance corresponds to a Nested-VRP problem in which the drone, with the same speed as the truck, observes 5 locations that are randomly generated by following uniform pattern.

Additional information is needed for solving the nested-VRP problem. First, battery capacity is set to 500 time units by default, which is enough for the drone to complete a round trip along the diagonal lines of the largest 2D plane across all instances from the small data set. Second, a single battery swap service takes 100 time units. Since the benchmark data does not provide any information about the observation times associated with locations, we randomly generate the observation times at each location by drawing uniformly from $[0, 250]$. In short, given a scenario characterized as (pattern, N , α), one of its instances is further characterized by observation times O for N locations, battery capacity T_{bl} , battery swap service time T_s ; and this is described as (pattern, N , α , O , T_{bl} , T_s). All the input data features are listed in Table 2.

Table 2: Summary of data features

Notations	Features	Values
P	patterns	{uniform, single-center, double-center}
N	number of locations	{ 5, 6, 7, 8, 9, 10 }
		{ 20, 50, 75, 100, 175, 250 }
T_{bl}	battery capacity	500
T_s	battery swap service time	100
O	observation time	Uniform[0, 250]
α	speed ratio of truck and drone	{ 1, 2, 3 }

By varying the shapes of the location pattern, the number of locations, and the speed ratios of the two vehicles, a total of $6 \times 3 \times 3 \times 10$ computational experiments were conducted on a computer with an Intel® Xeon® CPU E5-2687W v4 3.00 GHz processor and 64.0 GB installed RAM. All the algorithms and models are coded in Python 3.7, and the MIP model is solved via Gurobi 7.5.1. We limit Gurobi run-times to 15 minutes.

6.2. Small data set results

In this section, we solve in two ways the Nested-VRP problems for each instance contained in the small data set: via the MIP and via the NS heuristic. In Figure 5, we present the computational results obtained from solving instances belonging to uniform, single-center, and double-center scenarios. Detailed statistics are documented in Tables C.1, C.2, C.3, respectively, in Appendix C. Within each table, we report the results in three subgroups by differentiating $\alpha = \{1, 2, 3\}$. In particular, we record the average optimal mission makespan C_{MIP} and the average number of swap stops N_s in the resulting tours for instances belonging to the same scenario. Additionally, we track the optimality gap γ_{MIP} and run-times T_{MIP} reported from the Gurobi MIP solver. In Figure 5, we compare the performance of the NS

heuristic to the exact MIP approach by looking at the total number of instances where the optimal solutions are also obtained by the NS heuristic, N_{opt} , as well as the average run-times T_{NS} .

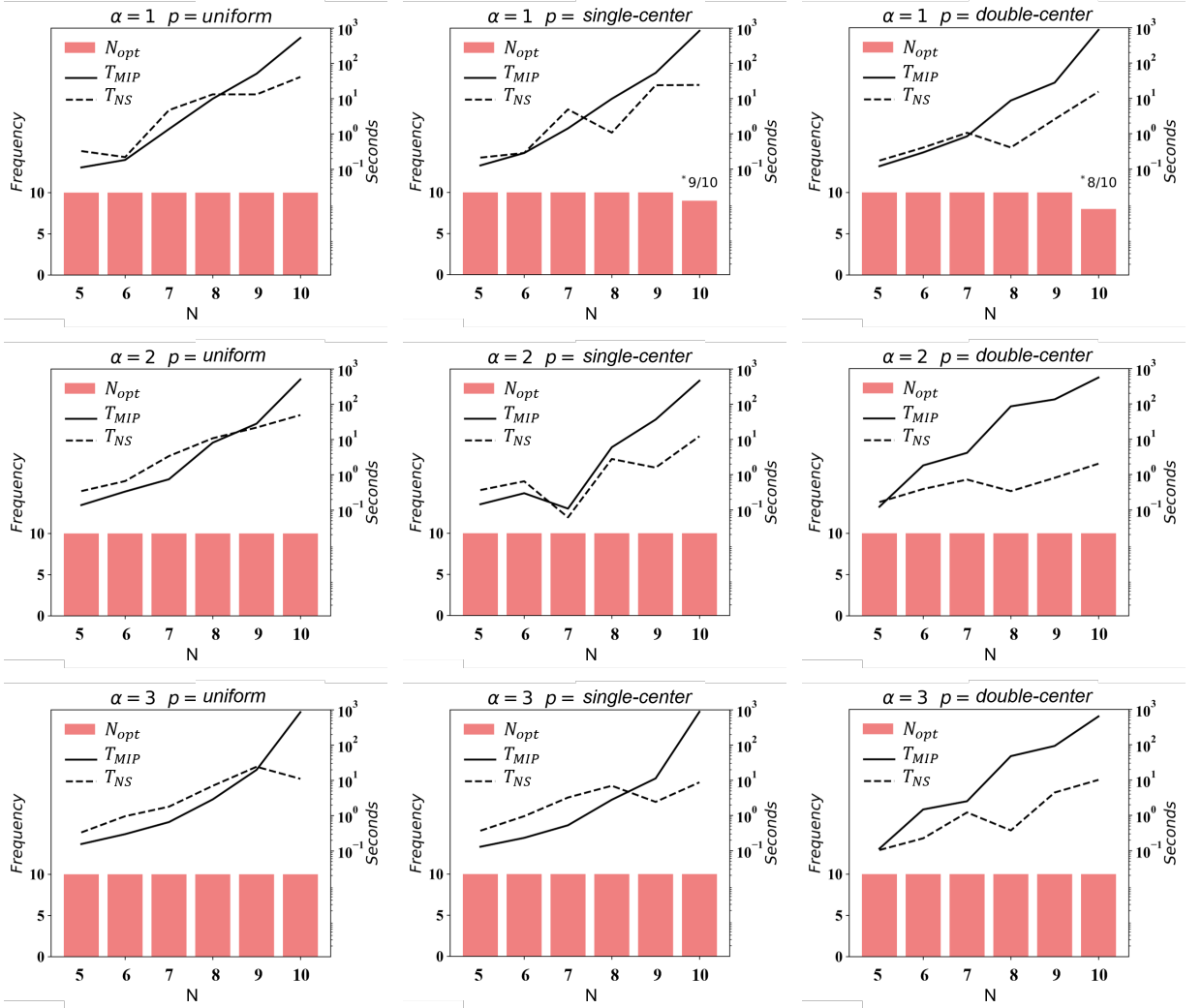


Figure 5: Frequency of optimal solutions found and comparison of run-times of the MIP exact approach and the NS heuristic. In a particular row, we consider the uniform, single-center, and double-center pattern shapes. In the vertical direction, we arrange the figures by increasing the speed ratio of the two vehicles from $\alpha = 1$ to $\alpha = 3$. In each subfigure, a red column corresponds to a scenario characterized by (pattern, N , α). Each scenario is based on the 10 instances provided by the benchmark dataset. Recall that for each scenario, N_{opt} counts the total number of instances where the optimal solutions are also obtained by the NS heuristic. Notably, the NS heuristic fails to find the optimal solutions for 1 instance in scenario (single-center, $N = 10$, $\alpha = 1$) and 2 instances in scenario (double-center, $N = 10$, $\alpha = 1$). In addition, the solid (dashed) line depicts the trend of computational time growth of the MIP approach (NS heuristic) as N increases.

First, we evaluate the quality of the MIP exact solutions. The MIP approach achieves a 0 gap within 15 minutes for all data instances except for scenarios (single-center, $N = 10$, $\alpha = 1$) and (double-center, $N = 10$, $\alpha = 1$). The difficulties in closing the gap come from the effects of the number of locations, the geometrical distribution of the locations, and the vehicles' speed ratio. We hypothesize that as the distribution of the locations becomes more skewed, the speed ratio between the two vehicles becomes more incompatible, and the size of the problem increases, then the drone experiences more difficulties in collaborating with the truck to replace batteries. From a computational complexity perspective, when solving the Nested-VRP model, finding the optimal solution requires an intensive search for the best combination of drone route, truck route, and battery swap locations. Therefore, the exact approach may

return a less-than-optimal solution given the run-time limit of 15 minutes. The loss of optimality due to the increased complexity of the problem has also been observed by González-Rodríguez et al. (2020), who solved a MIP model sharing similar features.

In terms of MIP computation time, when comparing our exact approach to that of González-Rodríguez et al. (2020), even though there is not much difference among instances of sizes $N \in \{6, 7, 8\}$, our MIP approach takes less than half of the run-times to solve cases involving $N = 9$ and $N = 10$. The observed improvement is a byproduct of Theorem 1. From these observations, we can conclude that our MIP approach has good performance when the problem size is relatively small.

Second, we investigate the relationship between vehicle speed ratios α and the mission makespan C_{MIP} . The purpose is to provide practical guidelines to pair a drone and a truck, with different speed settings, to achieve more operational efficiency. We do so by comparing the average percentage time savings (APTS) due to the change of vehicle speed ratio from α_1 to α_2 for a specific geometrical pattern p of interest. Given the pattern of interest $p \in \{\text{uniform, single-center, double-center}\}$, vehicle speed ratios of interest $\alpha_1, \alpha_2 \in \{1, 2, 3\}$, and possible number of locations $n \in \{5, 6, 7, 8, 9, 10\}$, let $C_{\text{MIP}}(p, n, \alpha_k), k \in \{1, 2\}$ denote the average mission makespan of scenario (pattern = $p, N = n, \alpha = \alpha_k$). Then, we can define $\text{APTS}(p, \alpha_1, \alpha_2)$ as follows.

$$\text{APTS}(p, \alpha_1, \alpha_2) \equiv \sum_{n \in \{5, 6, 7, 8, 9, 10\}} \frac{C_{\text{MIP}}(p, n, \alpha_2) - C_{\text{MIP}}(p, n, \alpha_1)}{6 C_{\text{MIP}}(p, n, \alpha_1)}$$

A more-negative $\text{APTS}(p, \alpha_1, \alpha_2)$ indicates that more time savings can be achieved by changing the speed ratio from α_1 to α_2 while the pattern p remains the same. Take the set of data from the uniform pattern as an example, in which case $\text{APTS}(\text{uniform}, 1, 2) = -6.806\%$ and $\text{APTS}(\text{uniform}, 1, 3) = -3.038\%$. In other words, increasing the vehicle speed ratio from 1 to 2 saves mission time by 6.806%. But further increasing the ratio from 2 to 3 will lose 3.768% of the savings that were already obtained. Thus, maintaining an appropriate, but not necessarily maximum, speed ratio between the two agents can improve operational efficiency.

Third, with regard to the performance of the NS heuristic, we have mixed signals. On one hand, we observe that the NS heuristic can find the optimal solution for each data instance whose optimal solution is achievable via the MIP approach. This is supported by the evidence in Figure 5. In the three cases where the optimal solutions are not available (see scenarios (single-center, $N = 10, \alpha = 1$) and (double-center, $N = 10, \alpha = 1$)), the NS heuristic finds difficulties in achieving the optimal solution as well. To further investigate if the solutions given by the NS heuristic are optimal or not, we solve the three mismatched instances using the MIP exact approach but relaxing the run-time limit to unbounded. The results show that in all three cases, the solutions returned by the NS heuristic are indeed aligned with the optimal solutions. Overall, we can conclude from the above observations that the NS heuristic is valid in solving problems of small size.

On the other hand, the run-times for obtaining an NS solution can be several times more expensive than those obtained via the exact approach. This phenomenon arises in cases where the initial feasible solution fed to the NS heuristic only contains a handful of nested units. Thus, the reconstruction process of each NS iteration is equivalent to re-solving almost but not exactly the original problem again. Moreover, this issue will be exacerbated when the total number of free locations to be reconstructed becomes larger during the reconstruction process. From the above discussion, we suggest leveraging the MIP exact approach when solving Nested-VRP of small/medium size. In the next section, we further examine how the NS heuristic performs when dealing with problems of larger size.

6.3. Large data set results

For solving larger-scale problems, we first perform the exact MIP approach via Gurobi with a 15-minute cutoff time. However, the MIP approach fails to provide satisfactory solutions. Therefore, we apply the NS heuristic to solve Nested-VRP problems involving large data sets. In the following experiments, the heuristic is parameterized by setting $K = 5$ and $N_{\text{max}} = 50$ as the termination criteria. To evaluate the quality of the solutions, we leverage the lower bound value introduced in §5.

Recall that the large data set considers locations of sizes $\{20, 50, 75, 100, 175, 250\}$ from uniform, single-center, and double-center geometrical patterns. Additionally, the speed ratio between the drone and the truck varies from $\{1, 2, 3\}$. Each scenario, characterized by (pattern, N, α), includes 10 instances.

Tables 3, 4, and 5 provide a comparison of the computational performance resulting from the application of various

different approaches on data from uniform, single-center, double-center patterns, respectively. Within a table, each row summarizes the statistics of interest per scenario. For each scenario, the statistics considered are:

- The average mission makespan of the solution obtained via Gurobi (15-minute cutoff time) $C_{15\text{mins}}$; via solving the CNU problem C_{CNU} (initialization of the NS Heuristic); and the NS heuristic C_{NS} .
- The estimate of the lower bound on mission makespan C_{lb} .
- The relative optimality gaps $\gamma_{15\text{mins}}, \gamma_{\text{CNU}}, \gamma_{\text{NS}}$ with respect to the estimate of the lower bound.
- For the NS heuristic, we also report the average run-times T_{NS} , number of iterations $\#_{\text{iter}}$, and number of recharge stops N_s .

Table 3: Results from solving instances from a uniform pattern in the large data set.

N	MIP	NS Heuristic					LB	Gap Comparison (%)		
	$C_{15\text{mins}}$	T_{NS}	$\#_{\text{iter}}$	N_s	C_{CNU}	C_{NS}	C_{lb}	$\gamma_{15\text{mins}}$	γ_{CNU}	γ_{NS}
$\alpha = 1$										
20	4345.0	10.0	5.3	7.4	4326.8	4225.5	4126.8	5.29	4.85	2.39
50	11961.0	8.5	4.8	18.7	9927.5	9893.3	9587.5	24.76	3.55	3.19
75	19381.0	5.7	5.5	28.3	14981.1	14821.7	14411.1	34.49	3.96	2.85
100	26278.0	9.9	7.2	35.6	19421.3	18899.8	18781.3	39.92	3.41	0.63
175	50957.0	32.1	5.6	65.4	34268.9	34028.8	33108.9	53.91	3.50	2.78
250	75790.0	17.5	5.5	92.5	48381.1	47255.7	46816.1	61.89	3.34	0.94
$\alpha = 2$										
20	5250.0	11.7	6.3	7.5	4708.6	4575.6	4488.6	16.96	4.90	1.94
50	13917.0	7.7	6.3	19.3	10883.7	10783.0	10503.7	32.50	3.62	2.66
75	21864.0	10.5	5.5	29.0	15532.2	15311.5	15012.2	45.64	3.46	1.99
100	35588.0	10.3	6.2	36.8	20150.7	19921.1	19500.7	82.50	3.33	2.16
175	63272.0	11.1	7.6	64.2	34954.8	34447.8	33894.8	86.67	3.13	1.63
250	87281.0	14.6	5.8	94.6	49981.3	49629.7	48386.3	80.38	3.30	2.57
$\alpha = 3$										
20	5139.0	4.1	6.0	8.2	5162.0	5004.7	4972.0	3.36	3.82	0.66
50	13917.0	3.0	6.3	21.1	11785.3	11618.4	11375.3	22.34	3.60	2.14
75	26040.0	7.0	7.2	28.6	16449.0	15965.7	15939.0	63.37	3.20	0.17
100	40659	3.7	7.0	38.9	21729.2	21088.8	21029.2	93.35	3.33	0.28
175	N/A	8.4	6.5	68.3	36631.3	35945.8	35471.3	N/A	3.27	1.34
250	N/A	17.1	7.0	94.4	50541.5	49728.1	49021.5	N/A	3.10	1.44

N/A: Solution is not available.

First, we explore the advantages of applying the proposed NS heuristic. As can be observed in column $\gamma_{15\text{mins}}$ in each of Tables 3–5, the MIP exact approach experiences difficulty in searching for the optimal solution and produces the best-known solution when the searching process is curtailed due to the limited run-time constraint. These incumbent solutions deviate substantially from the optimal solutions as the number of locations and the speed ratio between the two vehicles increase. The notation “N/A” indicates that Gurobi fails to return a feasible incumbent solution after 15 minutes of the search process. Compared to the MIP exact approach, the NS heuristic improves the solution quality by combining an effective initialization strategy and an effective local improvement scheme. To assess the effectiveness of the initialization strategy, when solving each Nested-VRP instance, we evaluate the relative optimality gap γ_{CNU} of the solution obtained by solving the CNU problem with respect to the lower bound value. The column γ_{CNU} suggests that solving the CNU problem produces robust feasible Nested-VRP solutions with a 3.63% average gap and a 0.59%

Table 4: Results from solving instances from a single-center pattern in the large data set.

N	MIP	NS Heuristic					LB	Gap Comparison (%)		
	C_{15mins}	T_{NS}	$\#_{iter}$	N_s	C_{CNU}	C_{NS}	C_{lb}	γ_{15mins}	γ_{CNU}	γ_{NS}
$\alpha = 1$										
20	4626.0	10.6	5.1	8.1	4471.8	4297.7	4281.8	8.04	4.44	0.37
50	12634.0	6.7	5.1	19.2	10382.4	10225.4	10002.4	26.31	3.80	2.23
75	18784.0	4.5	5.3	28.9	15357.4	15144.5	14817.4	26.77	3.64	2.21
100	29039.0	5.0	5.6	38.0	20367.3	20043.0	19687.3	47.50	3.45	1.81
175	48878.0	28.6	5.8	65.8	34490.6	34256.6	33330.6	46.65	3.48	2.78
250	N/A	24.6	5.8	92.9	48901.1	48436.2	47321.1	N/A	3.34	2.36
$\alpha = 2$										
20	5126.0	7.6	5.8	8.1	5175.9	4964.1	4935.9	3.85	4.86	0.57
50	14437.0	6.6	5.8	19.6	11053.6	10678.7	10653.6	35.51	3.75	0.24
75	23394.0	8.4	6.2	29.6	16424.1	16079.2	15854.1	47.56	3.60	1.42
100	33011.0	25.3	6.6	39.2	21729.5	21280.4	21079.5	56.60	3.08	0.95
175	62331.0	10.1	6.9	68.1	36872.8	36477.8	35742.8	74.39	3.16	2.06
250	N/A	27.3	6.9	96.0	51418.1	51010.3	49848.1	N/A	3.15	2.33
$\alpha = 3$										
20	6284.0	24.8	6.5	8.6	5914.1	5854.1	5664.1	10.94	4.41	3.35
50	14437.0	8.8	7.6	21.1	12533.5	12119.5	12093.5	19.38	3.64	0.21
75	23394.0	7.7	6.9	32.4	18212.1	17640.2	17612.1	32.83	3.41	0.16
100	41121.0	10.0	6.8	41.9	23598.2	23044.1	22898.2	79.58	3.06	0.64
175	N/A	11.9	7.4	73.0	39750.1	39118.1	38520.1	N/A	3.19	1.55
250	N/A	15.2	7.4	101.5	54744.7	54107.7	53029.7	N/A	3.23	2.03

N/A: Solution is not available.

standard deviation relative to the lower bound value C_{lb} across all large problems. We further examine the effectiveness of the pure local search process of the NS heuristic by assessing its contribution to optimality. By referring to columns γ_{CNU} and γ_{NS} , across all scenarios, the local search process contributes to a further 1.93% gap reduction on average given the initial feasible solution provided by solving the CNU problem.

It is also important to highlight that further reduction, obtained by the local search process, comes from exploring a relatively small number of nested units specified by the initial feasible solution. To see this, the number of battery swaps N_s is an indicator of the total number of nested units that are included in the final solution, while the number of iterations $\#_{iter}$ tells how many bad nested units are reorganized before reaching the final decision. As an example, in Table 5, in the scenario (double-center, $N = 250$, $\alpha = 3$), the NS heuristic takes on average 25.4 iterations to finalize the Nested-VRP solution, which consists of 105.05 nested units. Approximately 24.17% of the units are reorganized before the NS heuristic terminates. A similar analysis can be applied to other scenarios.

Second, we assess the quality of solutions provided by the NS heuristic. The NS heuristic is able to produce solutions with objective values that are reasonably close to the lower bound. Specifically, 25.93% of instances achieve results that deviate from the lower bound solution by less than 1%. Moreover, all instances can be solved within a 5% gap. It is worth noticing that the LB produces an over-optimistic estimation of the optimal value. Further tightening the LB will potentially gain more-accurate insights into the performance of the NS heuristic method.

Two observations can be made in terms of the NS's computation times. First, the time needed for NS to solve a Nested-VRP instance scales up reasonably as the total number of locations increases. For example, comparing the most-congested scenario (uniform, $N = 250$, $\alpha = 1$) to the least-congested scenario (uniform, $N = 5$, $\alpha = 1$), we find that the NS heuristic spends 53 times the latter's run-time in obtaining the Nested-VRP solution. However, the NS heuristic does not exhibit linear growth behavior in terms of run-times. This brings us to the second observation on

Table 5: Results from solving instances from a double-center pattern in the large data set.

N	MIP	NS Heuristic					LB	Gap Comparison (%)		
	C_{15mins}	T_{NS}	$\#_{iter}$	N_s	C_{CNU}	C_{NS}	C_{lb}	γ_{15mins}	γ_{CNU}	γ_{NS}
$\alpha = 1$										
20	5582.0	0.7	4.4	8.8	4812.2	4656.8	4592.2	21.55	4.79	1.41
50	13864.0	2.8	5.7	20.2	11150.8	10924.9	10750.8	28.96	3.72	1.62
75	24035.0	2.2	5.0	30.5	16159.6	15932.9	15529.6	54.77	4.06	2.60
100	36860.0	6.9	5.3	39.6	20993.2	20845.5	20303.2	81.55	3.40	2.67
175	69808.0	21.5	5.5	67.4	35488.9	35285.4	34328.9	103.35	3.38	2.79
250	N/A	22.3	5.9	95.1	49924.1	49713.8	48324.1	N/A	3.31	2.88
$\alpha = 2$										
20	6187.0	3.2	7.0	9.1	5868.8	5633.0	5548.8	11.50	5.77	1.52
50	14141.0	24.1	7.1	21.8	12711.6	12497.4	12281.6	15.14	3.50	1.76
75	28790.0	6.6	7.4	31.4	17934.6	17685.3	17304.6	66.37	3.64	2.20
100	46531.0	6.8	7.0	41.2	23018.8	22480.2	22288.8	108.76	3.28	0.86
175	N/A	11.4	6.4	72.8	39235.9	38453.1	38016.0	N/A	3.21	1.15
250	N/A	17.2	6.4	98.4	52798.0	51439.2	51228.6	N/A	3.06	0.41
$\alpha = 3$										
20	7516.0	1.4	7.8	9.5	6983.8	6778.2	6673.8	12.62	4.64	1.56
50	19599.0	1.2	8.0	22.8	14049.8	13845.9	13569.8	44.43	3.54	2.03
75	32526.0	5.6	7.2	34.6	19855.5	19573.9	19015.5	71.05	4.42	2.94
100	47173.0	15.8	10.1	42.0	25463.0	25063.9	24763.3	90.50	2.83	1.21
175	N/A	15.2	6.4	76.1	41464.3	40662.5	40214.4	N/A	3.11	1.11
250	N/A	16.6	8.0	105.1	57127.2	56427.05	55427.2	N/A	3.07	1.80

N/A: Solution is not available.

the growth of run-times. Suppose locations are scattered from the same pattern, and the speed ratio between vehicles is kept the same; then the NS heuristic computes its solution faster for a certain number of locations which we refer to as the “sweet spot”. As an example, consider a uniform pattern with $\alpha = 1$, in which case the “sweet spot” occurs at $N = 75$. Increasing or decreasing the number of locations, in this case, results in longer run-times required by the NS heuristic. This effect can be explained as follows. It is intuitive that when the density of locations increases, each nested unit in the solution may cover relatively more locations. Thus, the reconstruction process involves finding the exact solution to a larger Nested-VRP problem and drags down the computational run-times. Recall that the NS heuristic keeps identifying and reorganizing inefficient nested units. When the locations are relatively sparse, by nature, it is difficult to pack locations into one battery horizon while also satisfying the standard of efficiency. Thus, the NS heuristic wastes time in destructing and reorganizing nested units with the hope of improving battery efficiency. The “sweet spot” phenomenon reflects the complexity of the system.

To summarize the above discussion, the proposed NS heuristic is effective and efficient in producing high-quality solutions to the Nested-VRP problem.

6.4. Real-world case study

In this section, we focus on a realistic application of the Nested-VRP problem to surveillance in the aftermath of the 2017 Santa Rosa Wildfire. Our goal is to assess the effectiveness and efficiency of the NS heuristic in solving practical applications. Most importantly, we will further demonstrate the robustness of the proposed heuristic by empirically investigating its convergence behavior.

After the devastating fire disaster, an insurance company decided to send out a truck and a drone to inspect and collect home damage evidence from 631 clients’ properties. The information regarding all house locations is given. We set the truck speed as 5 m/s (considering the difficult ground conditions) and the drone speed as 10 m/s; thus, $\alpha = 2$.

The battery capacity is set to 10 minutes. The data cleaning process includes bundling observation tasks for apartments in the same building as a single observation task at the building's location. Correspondingly, the observation time is the sum of that for each apartment. We perform the NS heuristic on this specific instance for 100 independent runs to account for the randomness in the searching process. In each run, the NS heuristic will terminate if the program observes no improvements for $K = 5$ consecutive iterations or the total number of iterations exceeds $N_{\max} = 50$. We depict the best-known solution in Figure 6.

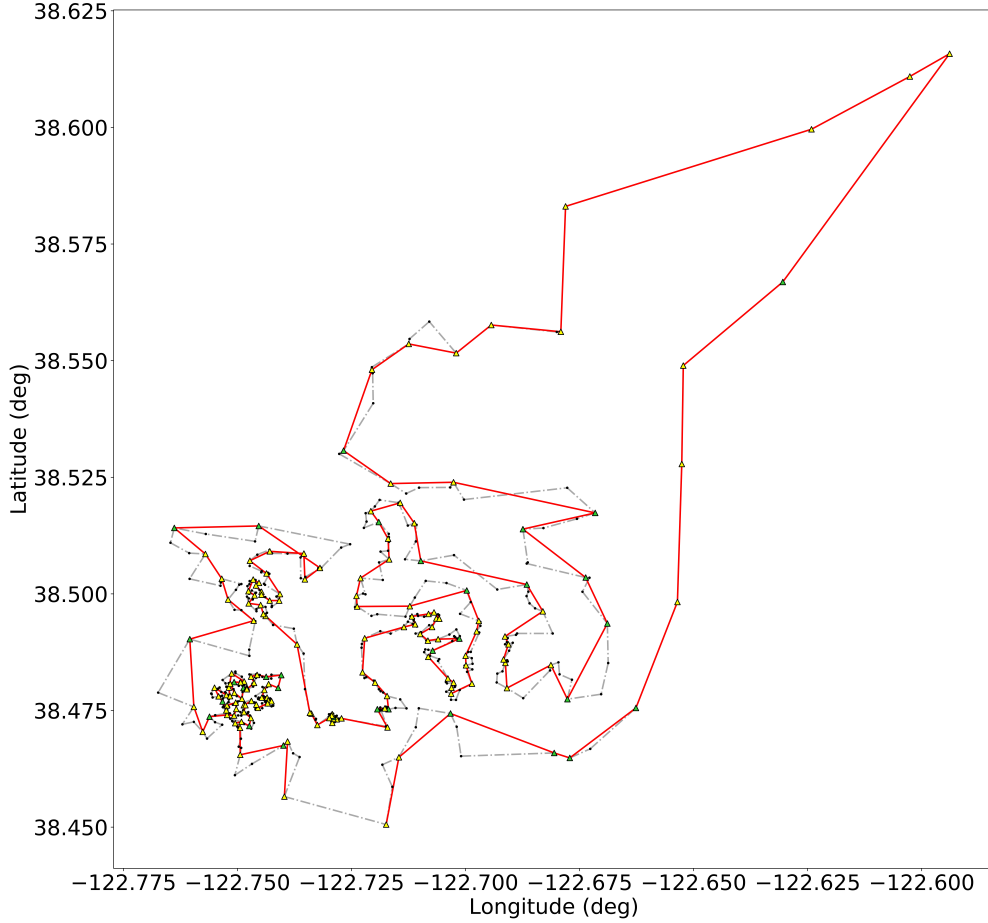


Figure 6: Nested-VRP solution for the practical instance. The red line is the truck route, while the grey line represents the drone route. Triangles depict the subset of locations serving as swap stops. Yellow and green colors differentiate the battery swaps that happen before or after the drone observes a location.

The best-known solution suggests that at least 26.29 hours are required to complete the entire mission, which consists of visiting 171 meet-up stops along the tour. We summarize the performance of the NS heuristic in Figure 7. In this figure, the i th blue box describes the distribution of γ_{NS} at the i th iteration across 100 runs. The average trend of γ_{NS} as the number of iteration increases is presented in the red curve. In addition, the green curve reports the average amount of time savings obtained per iteration.

Run-times: As the NS heuristic suggests, the average run-times for solving this Nested-VRP instance of size 631 is 645.7 seconds (10.76 minutes), which can be considered as efficient for planning a full-day mission.

Convergence: Referring to Figure 7, the red line summarizes its average trend across 100 runs. The red line suggests that the NS heuristic produces a Nested-VRP solution of smaller mission makespan as the local search process proceeds. Specifically, after solving the CNU model in the initialization stage, the NS heuristic produces a feasible Nested-VRP solution of 9.54% average optimality gap away from the estimate of lower bound value. Even though

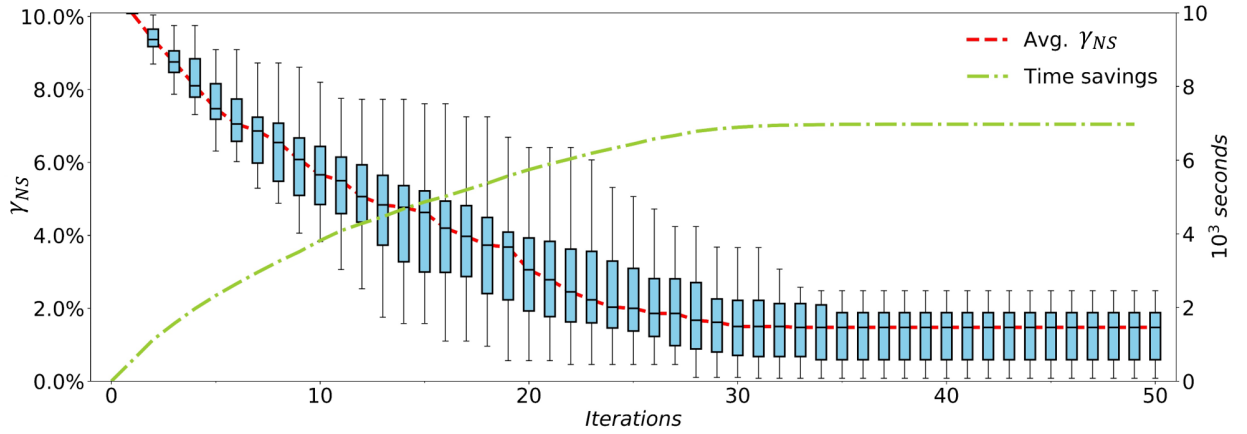


Figure 7: NS heuristic performance when solving the practical instance 100 times. The red line shows that the average optimality gap γ_{NS} decreases as the iteration number increases across the 100 tries. The green line shows that, compared to the mission makespan of the initial Nested-VRP solution obtained by solving CNU program, the NS heuristic finds a better solution via an effective local search scheme iteration by iteration. A better solution corresponds to a solution with a shorter mission makespan and thus corresponds to a larger time savings.

the red line has some “almost flat” segments (i.e., the 18th to 19th iterations), which indicate marginal improvement between iterations in the destruction and reconstruction process, these stationary stages were transient and eventually progressed to a better solution. This is evidence to show NS’s ability to escape local minima. Promisingly, the NS heuristic saves on average 7347.7 seconds (2.04 hours) from an initial CNU feasible solution and produces final results that are 1.47% closer to the lower bound on average.

It is worth noting that for a realistic Nested-VRP instance, implementing a drone-truck surveillance team to complete observation tasks may occasionally provide no time-saving benefits. Referring to Figure 6’s upper-right corner, we observe that the truck travels to multiple sites with the drone on-board. This is due to the geometrical configuration constituting the locations of the sites: relatively far away from each other and out of the drone’s reach from one location to the other. The solution is almost reduced to having a truck complete the surveillance task alone by following a partial TSP tour. In this case, the drone, even though it has the advantage of high cruising speed, does not contribute to speeding up the mission. Therefore, we lose the potential time-saving benefit of hiring a drone-truck surveillance team. This observation suggests that while matching the speed ratio between the truck and drone is crucial, picking the appropriate drone model with sufficient flight duration to support the mission is also important to the overall mission performance.

7. Conclusion

In this paper, the Nested-VRP problem is formally defined and formulated as a MIP program. Given the operational assumptions described in §3.1, our model is capable of finding the best trade-off between the drone’s routing plan and swap assignments along the route such that the total mission duration is minimized. In situations where the Gurobi solver fails to solve the Nested-VRP exactly, we further propose an NS heuristic approach that is based on destruction and local reconstruction principles. Our extensive experiments on small, large, and realistic instances have demonstrated the proposed heuristic’s ability to obtain reasonably good results while requiring substantially lower run-times compared to the MIP exact approach when the size of the problem is large.

Our empirical study has the following implications for future practitioners. (i) The geometrical distribution of the set of locations should be evaluated first to see the potential time-savings benefits that are achievable by implementing the drone-truck surveillance team. (ii) The speed of the two vehicles should be matched at the right ratio to maximize the overall time savings.

The model developed in this paper could enable a spectrum of applications in the field of aerial surveillance. Future work could include the ground traffic as a stochastic element into the model such that the ground delays will factor in the planning. In terms of algorithmic design, one might propose a sophisticated exact approach inspired by

branch-and-bound or a more-efficient heuristic that produces near-optimal solutions with reduced run-times. From a modeling perspective, while we only consider the case with a single truck and a single drone, one possible direction could be coordinating a team of drones together with multiple trucks to accomplish the goals and assessing the benefits of introducing more agents.

CRediT authorship contribution statement

Fanruiqi Zeng: Conceptualization, Methodology, Software, Investigation, Data Curation, Visualization, Writing – Original Draft. **Zaiwei Chen:** Conceptualization, Validation, Writing – Review & Editing. **John-Paul Clarke:** Conceptualization, Validation, Writing – Review & Editing, Supervision, Project administration. **David Goldsman:** Writing – Review & Editing, Supervision.

References

- Agatz, N., Bouman, P., and Schmidt, M. (2018). Optimization approaches for the traveling salesman problem with drone. *Transportation Science*, 52(4):965–981.
- Bouman, P., Agatz, N., and Schmidt, M. (2018). Dynamic programming approaches for the traveling salesman problem with drone. *Networks*, 72(4):528–542.
- Cakıcı, F., Ergezer, H., Irmak, U., and Leblebicioğlu, M. K. (2016). Coordinated guidance for multiple UAVs. *Transactions of the Institute of Measurement and Control*, 38(5):593–601.
- Cheng, C., Adulyasak, Y., and Rousseau, L.-M. (2018). *Formulations and Exact Algorithms for Drone Routing Problem*. CIRRELT, Interuniversity Research Center on Enterprise Networks, Logistics and Transportation.
- Daknama, R. and Kraus, E. (2017). Vehicle routing with drones. *arXiv preprint arXiv :1705.06431*.
- Dantzig, G., Fulkerson, R., and Johnson, S. (1954). Solution of a large-scale traveling-salesman problem. *Journal of the Operations Research Society of America*, 2(4):393–410.
- Dayarian, I., Savelsbergh, M., and Clarke, J.-P. (2020). Same-day delivery with drone resupply. *Transportation Science*, 54(1):229–249.
- De Freitas, J. C. and Penna, P. H. V. (2018). A randomized variable neighborhood descent heuristic to solve the flying sidekick traveling salesman problem. *Electronic Notes in Discrete Mathematics*, 66:95–102.
- Dell’Amico, M., Montemanni, R., and Novellani, S. (2019). Drone-assisted deliveries: New formulations for the flying sidekick traveling salesman problem. *Optimization Letters*, pages 1–32.
- Dorling, K., Heinrichs, J., Messier, G. G., and Magierowski, S. (2017). Vehicle routing problems for drone delivery. *IEEE Transactions on Systems, Man, and Cybernetics: Systems*, 47(1):70–85.
- González-Rodríguez, P. L., Canca, D., Andrade-Pineda, J. L., Calle, M., and Leon-Blanco, J. M. (2020). Truck-drone team logistics: A heuristic approach to multi-drop route planning. *Transportation Research Part C: Emerging Technologies*, 114:657–680.
- Ha, Q. M., Deville, Y., Pham, Q. D., and Ha, M. H. (2018). On the min-cost traveling salesman problem with drone. *Transportation Research Part C: Emerging Technologies*, 86:597–621.
- Karmarkar, N. (1984). A new polynomial-time algorithm for linear programming. In *Proceedings of the Sixteenth Annual ACM Symposium on Theory of Computing*, pages 302–311. Association for Computing Machinery, New York.
- Kitjacharoenchai, P., Ventresca, M., Moshref-Javadi, M., Lee, S., Tanchoco, J. M., and Brunese, P. A. (2019). Multiple traveling salesman problem with drones: Mathematical model and heuristic approach. *Computers & Industrial Engineering*, 129:14–30.
- Kulkarni, R. and Bhave, P. R. (1985). Integer programming formulations of vehicle routing problems. *European Journal of Operational Research*, 20(1):58–67.
- Laporte, G. (1992). The vehicle routing problem: An overview of exact and approximate algorithms. *European Journal of Operational Research*, 59(3):345–358.
- Lin, S. and Kernighan, B. W. (1973). An effective heuristic algorithm for the traveling-salesman problem. *Operations Research*, 21(2):498–516.
- Miao, Y., Zhong, L., Yin, Y., Zou, C., and Luo, Z. (2017). Research on dynamic task allocation for multiple unmanned aerial vehicles. *Transactions of the Institute of Measurement and Control*, 39(4):466–474.
- Miller, C. E., Tucker, A. W., and Zemlin, R. A. (1960). Integer programming formulation of traveling salesman problems. *Journal of the ACM (JACM)*, 7(4):326–329.
- Murray, C. C. and Chu, A. G. (2015). The flying sidekick traveling salesman problem: Optimization of drone-assisted parcel delivery. *Transportation Research Part C: Emerging Technologies*, 54:86–109.
- Murray, C. C. and Raj, R. (2020). The multiple flying sidekicks traveling salesman problem: Parcel delivery with multiple drones. *Transportation Research Part C: Emerging Technologies*, 110:368–398.
- Nemhauser, G. L. and Wolsey, L. A. (1999). *Integer and Combinatorial Optimization*, volume 55. John Wiley & Sons, New York.
- Poikonen, S. and Golden, B. (2020). The mothership and drone routing problem. *INFORMS Journal on Computing*, 32(2):249–262.
- Poikonen, S., Golden, B., and Wasil, E. A. (2019). A branch-and-bound approach to the traveling salesman problem with a drone. *INFORMS Journal on Computing*, 31(2):335–346.
- Raap, M., Meyer-Nieberg, S., Pickl, S., and Zsifkovits, M. (2017a). Aerial vehicle search-path optimization: A novel method for emergency operations. *Journal of Optimization Theory and Applications*, 172(3):965–983.
- Raap, M., Zsifkovits, M., and Pickl, S. (2017b). Trajectory optimization under kinematical constraints for moving target search. *Computers & Operations Research*, 88:324–331.

- Rego, C., Gamboa, D., Glover, F., and Osterman, C. (2011). Traveling salesman problem heuristics: Leading methods, implementations and latest advances. *European Journal of Operational Research*, 211(3):427–441.
- Sacramento, D., Pisinger, D., and Ropke, S. (2019). An adaptive large neighborhood search metaheuristic for the vehicle routing problem with drones. *Transportation Research Part C: Emerging Technologies*, 102:289–315.
- Schermer, D., Moeini, M., and Wendt, O. (2018). Algorithms for solving the vehicle routing problem with drones. In *Asian Conference on Intelligent Information and Database Systems*, pages 352–361. Springer, Cham.
- Schrijver, A. (1998). *Theory of Linear and Integer Programming*. John Wiley & Sons, New York.
- Shaw, P. (1998). Using constraint programming and local search methods to solve vehicle routing problems. In *International Conference on Principles and Practice of Constraint Programming*, pages 417–431. Springer.
- Tavana, M., Khalili-Damghani, K., Santos-Arteaga, F. J., and Zandi, M.-H. (2017). Drone shipping versus truck delivery in a cross-docking system with multiple fleets and products. *Expert Systems with Applications*, 72:93–107.
- Tokekar, P., Vander Hook, J., Mulla, D., and Isler, V. (2016). Sensor planning for a symbiotic UAV and UGV system for precision agriculture. *IEEE Transactions on Robotics*, 32(6):1498–1511.
- Toth, P. and Vigo, D. (2002). *The Vehicle Routing Problem*. Society for Industrial and Applied Mathematics, Philadelphia.
- Valente, J., Del Cerro, J., Barrientos, A., and Sanz, D. (2013). Aerial coverage optimization in precision agriculture management: A musical harmony inspired approach. *Computers and Electronics in Agriculture*, 99:153–159.

A. Proof of Theorem 1

PROOF. First, we set forth the ZONVRP formulation. Since there are no observations, we do not distinguish battery swaps that happen before or after observing a location. Therefore, for each location, we define $z_j \in \{0, 1\}, \forall j \in \mathcal{H}$. If $z_j = 1$, location j is a battery swap location. As a result, the time flow balance constraints (11), (15), (16) are replaced by constraints (28)–(30). Likewise, each location only requires a variable $l_j \in \mathcal{R}_+, \forall j \in \mathcal{H}$ to record the IBR time. Consequently, the IBR time constraints (19)–(24) are substituted by constraints (31)–(33).

$$t_j^+ = t_j^-(1 - z_j), \quad \forall j \in \mathcal{H} \quad (28)$$

$$t_j^- \leq t_i^+(1 - z_i) + \tau_{ij}^D - \tau_{ij}^D w_{ij} + M_1(1 - x_{ij}), \quad \forall (i, j) \in \mathcal{A} \quad (29)$$

$$t_j^- \geq t_i^+(1 - z_i) + \tau_{ij}^D - \tau_{ij}^D w_{ij} - M_1(1 - x_{ij}), \quad \forall (i, j) \in \mathcal{A} \quad (30)$$

$$l_j \leq z_j T_{bl}, \quad \forall j \in \mathcal{H} \quad (31)$$

$$t_j^- - T_{bl} \sum_{i:(i,j) \in \mathcal{A}} w_{ij} \leq l_j + M_1(1 - z_j), \quad \forall j \in \mathcal{H} \quad (32)$$

$$\sum_{i:(i,j) \in \mathcal{A}} \tau_{ij}^T y_{ij} \leq l_j + M_2(1 - z_j), \quad \forall j \in \mathcal{H} \quad (33)$$

The ZONVRP model is presented as follows:

$$\begin{aligned} (\text{ZONVRP}) \quad & \min \sum_{i \in \mathcal{H}} l_i + \gamma \sum_{(i,j) \in \mathcal{A}} q_{ij} \\ \text{s.t.} \quad & \text{constraints: (1)–(10), (12)–(14), (17)–(18), (28)–(33)} \\ & z_0 = 1, t_0^+ = 0 \\ & x_{ij} \in \{0, 1\}, y_{ij} \in \{0, 1\}, w_{ij} \in \{0, 1\}, q_{ij} \in \mathcal{R}_+, \quad \forall (i, j) \in \mathcal{A} \\ & z_i \in \{0, 1\}, u_i \in [0, n+1], t_i^-, t_i^+ \in [0, T_{bl}], l_i \in \mathcal{R}_+, \quad \forall i \in \mathcal{H} \end{aligned}$$

We use the notation $\text{TDTL}(k)$ to refer to the k -th constraint in the TDTL model in González-Rodríguez et al. (2020). Let the polyhedron of the linear relaxation of models ZONVRP and TDTL be defined by

$$\begin{aligned} P(\text{TDTL}) &= \left\{ (s, b^-, b^+, u, v) \in \mathcal{R}_{\geq 0}^{3(n+1)} \times [0, 1]^{2n^2} \mid \text{constraints: TDTL.(2)–TDTL.(25)} \right\} \\ P(\text{ZONVRP}) &= \left\{ (l, t^-, t^+, z, u, q, w, x, y) \in \mathcal{R}_{\geq 0}^{5(n+1)} \times [0, 1]^{4n^2} \mid \right. \\ &\quad \left. \text{constraints: (1)–(10), (12)–(14), (17)–(18), (28)–(33)} \right\} \end{aligned}$$

Given the linear transformation Φ in (34)–(39) below, we will show that each constraint in $P(\text{TDTL})$ is implied by that in $P(\text{ZONVRP})$.

$$x_{ij} = v_{ij} \quad (34)$$

$$y_{ij} = u_{ij} \quad (35)$$

$$z_j = \sum_{i:(i,j) \in \mathcal{A}} u_{ij} \quad (36)$$

$$t_i^- = Q - b_i^- \quad (37)$$

$$t_i^+ = Q - b_i^+ \quad (38)$$

$$l_j + t_j^- - t_i^+ = s_j - s_i \quad (39)$$

TDTL.(2)

$$\sum_{i:(i,j) \in \mathcal{A}} u_{ij} = z_j \leq 1$$

TDTL.(3) is implied by constraint (7).

TDTL.(4) and (5) are implied by constraint (6) directly.

TDTL.(6)–(9) are implied by constraints (1)–(2) directly.

TDTL.(10)

$$\sum_{i:(i,j) \in \mathcal{A}} u_{ij} + \sum_{i:(i,j) \in \mathcal{A}} v_{ij} = z_j + \sum_{i:(i,j) \in \mathcal{A}} x_{ij} = z_j + 1 \geq 1$$

TDTL.(11) is in charge of setting the departure time at node j given that arc (i, j) is traversed by the truck.

$$\begin{aligned} & s_j - s_i - t_{ij}^T u_{ij} + M(1 - u_{ij}) \\ &= l_j + t_j^- - t_i^+ - \tau_{ij}^T y_{ij} + M(1 - y_{ij}) \\ &\geq l_j + t_j^- - t_i^+ - \tau_{ij}^T, \quad \text{implied by } y_{ij} = 1 \\ &= (l_j - \tau_{ij}^T) + (t_j^- - t_i^+) \\ &\geq 0 \end{aligned}$$

TDTL.(12) regulates the departure time at node j given that arc (i, j) is traversed by the drone.

$$\begin{aligned} & s_j - s_i - t_{ij}^D u_{ij} + M(1 - v_{ij} + u_{ij}) \\ &= l_j + t_j^- - t_i^+ - \tau_{ij}^D x_{ij} + M(1 - x_{ij} + y_{ij}) \\ &\geq l_j + t_j^- - t_i^+ - \tau_{ij}^D, \quad \text{implied by } x_{ij} = 1, y_{ij} = 0 \\ &= (l_j - \tau_{ij}^D) + (t_j^- - t_i^+) \\ &\geq 0 \end{aligned}$$

TDTL.(14)–(17) describe the drone's battery level at the time it just arrives at or departs from a node j .

$$\begin{aligned} & b_j^- - Q - M(2 - v_{ij} - u_{ij}) = -t_j^- - M(2 - x_{ij} - y_{ij}) \leq 0 \\ & b_j^- - Q + M(2 - v_{ij} - u_{ij}) = -t_j^- + M(2 - x_{ij} - y_{ij}) \geq 0, \quad \text{implied by constraints (7), (14), (29)–(30)} \\ & b_j^+ - Q - M(2 - v_{ij} - u_{ij}) = -t_j^+ - M(2 - x_{ij} - y_{ij}) \leq 0 \\ & b_j^+ - Q + M(2 - v_{ij} - u_{ij}) = -t_j^+ + M(2 - x_{ij} - y_{ij}) \geq 0, \quad \text{implied by constraints (7), (14), (28)–(30)} \end{aligned}$$

TDTL.(18), $\forall(i, j) \in \mathcal{A}$

$$\begin{aligned}
& b_j^- - b_i^+ + \tau_{ij}^D - M \left(1 - v_{ij} + u_{ij} + \sum_{k \neq i} u_{kj} \right) \\
&= t_i^+ - t_j^- + \tau_{ij}^D - M(1 - x_{ij} + z_j) \\
&\leq t_i^+ z_i + \tau_{ij}^D w_{ij} + M(1 - x_{ij}) - M(1 - x_{ij} + z_j), \quad \text{implied by constraint (30)} \\
&= t_i^+ z_i + \tau_{ij}^D w_{ij} - M z_j \\
&= t_i^-(1 - z_i) z_i + \tau_{ij}^D w_{ij} - M z_j, \quad \text{implied by constraint (28)} \\
&\leq 0, \quad \text{implied by } z_j = 0
\end{aligned}$$

TDTL.(19), $\forall(i, j) \in \mathcal{A}$

$$\begin{aligned}
& b_j^- - b_i^+ + \tau_{ij}^D + M \left(1 - v_{ij} + u_{ij} + \sum_{k \neq i} u_{kj} \right) \\
&= t_i^+ - t_j^- + \tau_{ij}^D + M(1 - x_{ij} + z_j) \\
&\geq t_i^+ z_i + \tau_{ij}^D w_{ij} - M(1 - x_{ij}) + M(1 - x_{ij} + z_j), \quad \text{implied by constraint (29)} \\
&= t_i^-(1 - z_i) z_i + \tau_{ij}^D w_{ij} + M z_j \\
&\geq 0, \quad \text{implied by } z_j = 0
\end{aligned}$$

TDTL.(20), $\forall(i, j) \in \mathcal{A}$

$$\begin{aligned}
& b_j^+ - b_j^- - M \left(1 - v_{ij} + u_{ij} + \sum_{k \neq i} u_{kj} \right) \\
&= Q - t_j^+ - Q + t_j^- - M(1 - x_{ij} + z_j) \\
&= t_j^- z_j - M(1 - x_{ij} + z_j) \\
&\leq 0, \quad \text{implied by constraint (29)}
\end{aligned}$$

TDTL.(21), $\forall(i, j) \in \mathcal{A}$

$$\begin{aligned}
& b_j^+ - b_j^- + M \left(1 - v_{ij} + u_{ij} + \sum_{k \neq i} u_{kj} \right) \\
&= t_j^- z_j + M(1 - x_{ij} + z_j) \\
&\geq 0, \quad \text{implied by } x_{ij} = 1, z_j = 0
\end{aligned}$$

TDTL.(22)

$$\begin{aligned}
& b_j^- - b_i^+ + \tau_{ij}^D - M \left(1 - v_{ij} + u_{ij} + 1 - \sum_{k \neq i} u_{kj} \right) \\
&= -t_j^- + t_i^+ + \tau_{ij}^D - M \left(1 - x_{ij} + y_{ij} + 1 - \sum_{k \neq i} y_{kj} \right) \\
&\leq t_i^+ z_i + \tau_{ij}^D w_{ij} + M(1 - x_{ij}) - M \left(1 - x_{ij} + y_{ij} + 1 - \sum_{k \neq i} y_{kj} \right), \quad \text{implied by constraint (30)} \\
&= t_i^-(1 - z_i) z_i + \tau_{ij}^D w_{ij} - M \left(y_{ij} + 1 - \sum_{k \neq i} y_{kj} \right) \\
&\leq 0, \quad \text{implied by } y_{ij} = 0, \sum_{k \neq i} y_{kj} = 1, \text{ constraint (14)}
\end{aligned}$$

TDTL.(23), $\forall(i, j) \in \mathcal{A}$

$$\begin{aligned}
& b_j^- - b_i^+ + \tau_{ij}^D + M \left(1 - v_{ij} + u_{ij} + 1 - \sum_{k \neq i} u_{kj} \right) \\
& = -t_j^- + t_i^+ + \tau_{ij}^D + M \left(1 - x_{ij} + y_{ij} + 1 - \sum_{k \neq i} y_{kj} \right) \\
& \geq t_i^+ z_i + \tau_{ij}^D w_{ij} - M(1 - x_{ij}) + M \left(1 - x_{ij} + y_{ij} + 1 - \sum_{k \neq i} y_{kj} \right), \quad \text{implied by constraint (30)} \\
& = t_i^-(1 - z_i) z_i + \tau_{ij}^D w_{ij} + M \left(y_{ij} + 1 - \sum_{k \neq i} y_{kj} \right), \quad \text{implied by constraint (28)} \\
& \geq 0, \quad \text{implied by } y_{ij} = 0, \sum_{k \neq i} y_{kj} = 1
\end{aligned}$$

TDTL.(24), $\forall(i, j) \in \mathcal{A}$

$$\begin{aligned}
& b_j^+ - Q - M \left(1 - v_{ij} + u_{ij} + 1 - \sum_{k \neq i} u_{kj} \right) \\
& = -t_j^+ - M \left(1 - x_{ij} + y_{ij} + 1 - \sum_{k \neq i} y_{kj} \right) \\
& \leq 0
\end{aligned}$$

TDTL.(25), $\forall(i, j) \in \mathcal{A}$

$$\begin{aligned}
& b_j^+ - Q + M \left(1 - v_{ij} + u_{ij} + 1 - \sum_{k \neq i} u_{kj} \right) \\
& = -t_j^+ + M \left(1 - x_{ij} + y_{ij} + 1 - \sum_{k \neq i} y_{kj} \right) \\
& = -t_j^-(1 - z_j) \\
& \geq 0, \quad \text{implied by } x_{ij} = 1, y_{ij} = 0, \sum_{k \neq i} y_{kj} = 1
\end{aligned}$$

We have finally shown that $\Phi(P(\text{ZONVRP})) \subseteq P(\text{TDTL})$. To further establish that the feasible region of $\Phi(P(\text{ZONVRP}))$ is strictly contained in $P(\text{TDTL})$, it is sufficient to give a solution that is valid in TDTL model but infeasible in ZONVRP model.

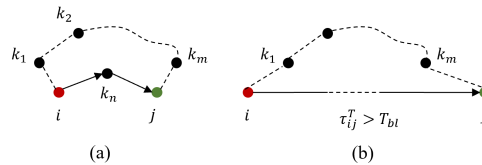


Figure A.1: Partial solutions that are avoided in ZONVRP.

In Figure A.1 (a), we depict a nested unit in which the truck visits location k_n before drives to rendezvous location j . This nested unit could be part of any TDTL solution. However, such solution is infeasible to the ZONVRP model since constraints (1)–(2) require that each location has to be visited by the drone exactly once. In this case shown in Figure A.1 (b), the truck travels for more than T_{bl} time units to the designated destination j ; and here the drone has depleted its battery and has been forced to land on the ground. But the ZONVRP excludes this situation via the constraint (10). \square

B. Proof of Theorem 3

PROOF. Given a Nested-VRP problem described in graph $\mathcal{G} = (\mathcal{H}, \mathcal{A})$, the optimal solution to the problem consists of the drone route $\mathcal{X} = \{(i, j) \mid (i, j) \in \mathcal{A}, \text{ and } x_{ij} = 1\}$ and the truck route $\mathcal{Y} = \{(i, j) \mid (i, j) \in \mathcal{A}, \text{ and } y_{ij} = 1\}$. The optimal solution can also be described as a set of non-overlapping nested units U . Mathematically, a nested unit $u \in U$ can be viewed as a sub-graph of \mathcal{G} . The sub graph contains a set of locations $V(u)$ to be observed by the drone and the corresponding drone path $E(u)$. Most importantly, one can see that $\mathcal{X} \equiv \{(i, j) \mid (i, j) \in E(u), u \in U\}$ and $\mathcal{H} \equiv \{k \mid k \in V(u), u \in U\}$.

In a nested unit u , when the drone is about to meet with the truck, the drone arrives at the rendezvous location either earlier than the truck and idles for Δ_u time units or later than the truck without idling. We define an indicator function $\mathbb{1}_u$ for each nested unit u that forms the optimal Nested-VRP solution. In a nested unit u , if the drone arrives earlier than the truck at rendezvous, $\mathbb{1}_u = 1$, otherwise $\mathbb{1}_u = 0$. After two vehicles meet up successfully, the drone relinquishes all remaining battery life before it obtains a new battery. This portion of unused battery life is denoted as δ_u .

A battery is either used for drone surveillance (e.g., routing between locations, surveying locations, and possibly waiting for the truck) or wasted after the two vehicles meet up. To derive the lower bound of the mission makespan of a Nested-VRP solution, we first investigate the battery consumption associated with a Nested-VRP solution. Denote the IBR l_u of a nested unit as in Equation (40). We summarize the battery consumption breakdowns in Equation (41).

$$l_u = \sum_{(i,j) \in E(u)} \tau_{ij}^D x_{ij} + \sum_{k \in V(u)} o_k + \mathbb{1}_u \Delta_u \quad (40)$$

$$T_{bl} = l_u + \delta_u \quad (41)$$

Due to the conservation of energy, the amount of energy extracted from all battery replacements scheduled en route should be able to balance off the total battery consumption needed for the mission. Therefore, we can derive the necessary number of battery swaps N_s as follows:

$$N_s T_{bl} = \sum_{u \in U} (l_u + \delta_u) = \sum_{u \in U} \left(\sum_{(i,j) \in E(u)} \tau_{ij}^D x_{ij} + \sum_{k \in V(u)} o_k + \mathbb{1}_u \Delta_u + \delta_u \right)$$

$$N_s = \frac{1}{T_{bl}} \sum_{u \in U} \left(\sum_{(i,j) \in E(u)} \tau_{ij}^D x_{ij} + \sum_{k \in V(u)} o_k + \mathbb{1}_u \Delta_u + \delta_u \right)$$

Since the mission makespan is the sum of the IBRs $l_u, \forall u \in U$ and battery swap service times:

$$\begin{aligned} \text{makespan} &= \sum_{u \in U} l_u + N_s T_s \\ &= \sum_{u \in U} \left(\sum_{(i,j) \in E(u)} \tau_{ij}^D x_{ij} + \sum_{k \in V(u)} o_k + \mathbb{1}_u \Delta_u \right) + \frac{T_s}{T_{bl}} \sum_{u \in U} \left(\sum_{(i,j) \in E(u)} \tau_{ij}^D x_{ij} + \sum_{k \in V(u)} o_k + \mathbb{1}_u \Delta_u + \delta_u \right) \end{aligned}$$

We relax constraints imposed on how battery swap could happen and allow the drone to charge itself at any time when its battery has depleted. Therefore, the mission makespan of a relaxed version of Nested-VRP instance is given by:

$$\begin{aligned} \text{makespan} &= \sum_{u \in U} \left(\sum_{(i,j) \in E(u)} \tau_{ij}^D x_{ij} + \sum_{k \in V(u)} o_k \right) + \frac{T_s}{T_{bl}} \sum_{u \in U} \left(\sum_{(i,j) \in E(u)} \tau_{ij}^D x_{ij} + \sum_{k \in V(u)} o_k \right) \\ &= \sum_{(i,j) \in \mathcal{X}} \tau_{ij}^D x_{ij} + \sum_{k \in \mathcal{H}} o_k + \frac{T_s}{T_{bl}} \left(\sum_{(i,j) \in \mathcal{X}} \tau_{ij}^D x_{ij} + \sum_{k \in \mathcal{H}} o_k \right) \quad (42) \end{aligned}$$

$$\geq \sum_{(i,j) \in S} \tau_{ij}^D + \sum_{k \in \mathcal{H}} o_k + \lfloor \frac{1}{T_{bl}} \left(\sum_{(i,j) \in S} \tau_{ij}^D + \sum_{k \in \mathcal{H}} o_k \right) \rfloor T_s, \quad (43)$$

Recall that S is the collection of arcs that are in the TSP route. Since the union of the drone paths in all nested

units will produce a Hamiltonian cycle containing all of the locations and whose total length is no shorter than the TSP route, Equation (42) will be lower bounded by specifying the drone route as the TSP route as well as rounding down the total number of battery swaps to an integer. The result is that, the objective function value of the original Nested-VRP model is lower bounded by term (43). \square

C. Computational results on small data set

Table C.1: Results from solving instances from the uniform pattern in the small data set.

uniform	MIP					NS Heuristic	
	N	C_{MIP}	N_s	γ_{MIP}	T_{MIP}	N_{opt}	T_{NS}
$\alpha = 1$							
	5	891.8	1.5	0	0.11	10/10	0.33
	6	469.2	1.2	0	0.18	10/10	0.22
	7	1473.8	2.6	0	1.37	10/10	4.72
	8	1596.2	2.9	0	9.96	10/10	13.24
	9	1759.6	3.3	0	51.01	10/10	13.20
	10	1986.7	3.6	0	529.20	10/10	41.31
$\alpha = 2$							
	5	1086.6	2.3	0	0.14	10/10	0.34
	6	1259.9	2.5	0	0.33	10/10	0.66
	7	1246.6	3.1	0	0.75	10/10	3.38
	8	1351.4	3.6	0	8.13	10/10	10.85
	9	1530.5	3.8	0	28.13	10/10	21.84
	10	1501.6	4.3	0	505.66	10/10	49.37
$\alpha = 3$							
	5	1080.3	2	0	0.16	10/10	0.33
	6	1215.8	2.1	0	0.30	10/10	0.96
	7	1394.7	3.1	0	0.65	10/10	1.79
	8	1432.4	3.4	0	2.88	10/10	6.99
	9	1571	4.5	0	19.85	10/10	24.30
	10	1718.2	4.5	0	857.76	10/10	11.05

Table C.2: Results from solving instances from the single-center pattern in the small data set.

single-center	MIP					NS Heuristics	
	N	C_{MIP}	N_s	γ_{MIP}	T_{MIP}	N_{opt}	T_{NS}
$\alpha = 1$							
5	1173.4	2.2	0	0.13	10/10	0.21	
6	1426.8	2.5	0	0.28	10/10	0.285	
7	1292	2.4	0	1.42	10/10	4.918	
8	1622	2.8	0	9.85	10/10	1.077	
9	1942.2	3.6	0	53.59	10/10	23.868	
10	2133.1	3.9	0.017	840.88	9/10	24.334	
$\alpha = 2$							
5	1022	1.9	0	0.14	10/10	0.364	
6	1204.5	3	0	0.30	10/10	0.646	
7	1657.2	3.4	0	0.11	10/10	0.061	
8	1443.6	3.6	0	5.98	10/10	2.78	
9	1611.8	3.5	0	36.63	10/10	1.579	
10	1766.4	3.1	0	464.30	10/10	12.274	
$\alpha = 3$							
5	1073.4	2.1	0	0.13	10/10	0.368	
6	1291.4	2.4	0	0.23	10/10	0.953	
7	1285.4	2.9	0	0.53	10/10	3.234	
8	1486.5	3.4	0	2.80	10/10	6.967	
9	1732.5	3.5	0	11.29	10/10	2.427	
10	1853.6	4.1	0	880.89	10/10	11.718	

Table C.3: Results from solving instances from the double-center pattern in the small data set.

double-center	MIP					NS Heuristics	
	N	C_{MIP}	N_s	γ_{MIP}	T_{MIP}	N_{opt}	T_{NS}
$\alpha = 1$							
5	1371.1	2.3	0	0.12	10/10	0.17	
6	1411.3	2.1	0	2.94	10/10	0.40	
7	1778.5	3	0	8.4	10/10	1.06	
8	1898.8	3.4	0	86.93	10/10	0.41	
9	2122.8	3.5	0	278.56	10/10	2.56	
10	2429.4	4.2	0.032	870.03	8/10	15.44	
$\alpha = 2$							
5	1375.7	2.6	0	0.122	10/10	0.17	
6	1608.2	3.1	0	1.81	10/10	0.39	
7	1565	2.8	0	4.11	10/10	0.72	
8	1831.4	3.2	0	85.2	10/10	0.34	
9	1909.8	3.6	0	134.1	10/10	0.80	
10	2126	4.1	0	558.26	10/10	2.03	
$\alpha = 3$							
5	1446.8	2.7	0	0.114	10/10	0.10	
6	1525.9	2.9	0	1.47	10/10	0.22	
7	1705.1	3.2	0	2.51	10/10	1.21	
8	1883.9	3.6	0	47.5	10/10	0.37	
9	1901.3	3.9	0	92.44	10/10	4.43	
10	2312.716	4.5	0	634.76	10/10	10.12	